Connection between kinetic methods for fluid-dynamic equations and macroscopic finite-difference schemes

Connection between kinetic methods for fluid-dynamic equations and macroscopic finite-difference schemes

Pietro Asinari [a] and Taku Ohwada [b]

[a] *Dipartimento di Energetica, Politecnico di Torino, Torino 10129, Italy*

[b] *Department of Aeronautics and Astronautics, Graduate School of Engineering, Kyoto University, Kyoto 606-8501, Japan*

Abstract

The lattice Boltzmann method (LBM) for the incompressible Navier-Stokes (NS) equations and the gas kinetic scheme for the compressible NS equations are based on the kinetic theory of gases. In the latter case, however, it is shown that the kinetic formulation is necessary only in the discontinuous reconstruction of fluid-dynamic variables for shock capturing. Analogously we will discuss the reduction of a kinetic method for the incompressible case, where the LBM scheme will be shown to shrink to an artificial compressibility type finite-difference scheme. We will prove first that a simple and compact LBM scheme can not catch rarefied effects beyond Navier-Stokes and hence that it is worth the effort to develop kinetic-based FD alternatives. Finally we will propose two improvements to existing kinetic-based FD schemes: first of all, (a) the proposed scheme is formulated purely in terms of macroscopic quantities on a compact stencil; secondly (b) the semi-implicit formulation is proposed in order to increase the stability. We think that this work may be useful to others in realizing the actual possibilities of simple LBM schemes beyond Navier-Stokes and in adopting the suggested improvements in their actual FD codes.

Key words: incompressible flow, artificial compressibility, asymptotic analysis, lattice Boltzmann method

1 INTRODUCTION

In the last years, the lattice Boltzmann method (LBM) has become very popular among the discretization techniques for solving PDE systems in fluid-dynamics, such as the incompressible Navier-Stokes equations. Starting from

some pioneer works [1, 2, 3], the method has reached a more systematic fashion [4, 5] by means of a better understanding of the connections with the continuous kinetic theory [6, 7]. A more complete and recent coverage of various previous contributions on LBM can be found in some books [8, 9, 10] and some review papers [11, 12].

The lattice kinetic scheme (LKS) [13, 14], which is a variant of LBM, employs a simpler updating rule of the distribution function than the original LBM. The updated distribution function is given by the linear combination of the equilibrium distribution function at each point of the stencil. Since the equilibrium function is characterized by macroscopic variables, it is obvious from this updating rule that LKS deals with only macroscopic variables in the actual computation. In fact, the similarity of LBM with the artificial compressibility method (ACM) proposed by Chorin [15] is discussed by using LKS in Ref. [14]. For artificial compressibility method we intend a system of equations derived by incompressible Navier-Stokes system by adding to the divergence-free condition for the velocity field a term which is linearly proportional to the time derivative of the pressure. LKS has the similarity with another well-known kinetic CFD tool called Gas Kinetic Scheme (GKS). GKS employs truncated asymptotic solutions of kinetic equations for small Knudsen numbers, e.g. the local Maxwellian is employed in Pullin's equilibrium flux method for the compressible Euler equations [16] and its first order correction in the Chapman-Enskog expansion is done in Kinetic Flux Vector Splitting of Chou and Baganoff for the compressible Navier-Stokes equations [17]. Thus, the actual computation of GKS requires only the macroscopic data as in the case of LKS, which is in contrast to the original LBM. For this reason, one may think that the original LBM has a more promising potential ability to deal with higher rarefaction effect correctly than GKS and LKS. On the other hand, the recent theoretical studies of GKS [18, 19, 20] reveal that the outcome of kinetic formulation of numerical methods for the compressible Euler and Navier-Stokes systems lies only in a simple treatment of discontinuous reconstruction of macroscopic variables for shock-capturing; the linearity of convective term of kinetic equation yields a drastic simplification of theory of approximate Riemann solver. Needless to say, the main target fluid of LBM is incompressible and continuous, where LBM is not required to have the same outcome of kinetic formulation as that of GKS.

In the present study, we investigate the outcome of kinetic formulation of LBM theoretically and numerically. The main purpose of the paper is to make the LBM users recognize the effective nature of LBM and appreciate the outcome of the simple modification based on this fact. We found that LBM scheme shrinks to an artificial compressibility type finite-difference scheme. The asymptotic techniques for recovering the macroscopic equations solved by LBM at macroscopic level are well know, both traditional ones (Chapman-Enskog) and systematic ones (Hilbert). Many papers exist about this topic.

However we want to point out some properties of the macroscopic system of equations recovered by LBM and used to solve incompressible Navier-Stokes, more than the way we used to derive it, i.e. the LBM itself. With other words, at macroscopic level, we found a system of equations which is close to that considered by the Chorin's artificial compressibility method, but with a mesh dependent parameter. Introducing a mesh dependent parameter in front of the compressible term makes a non-trivial difference and it opens new room for improvements.

The organization of the paper is as follows. In Sec. 2, we discuss the perspective of realization of LBM computation beyond Navier-Stokes. For this purpose, we carry out the asymptotic analysis of continuous BGK equation (Hilbert expansion) and the similar asymptotic analysis of lattice-BGK method according to the recipe of Ref. [21], where the asymptotic behavior of MRT LBM is studied. The employment of lattice-BGK is for the simplicity in dealing with higher order kinetic effects beyond Navier-Stokes. The equation systems derived in the asymptotic analysis are summing up and the resulting equation system is discussed. The principal part of the resulting equation system is in the same form as Chorin's artificial compressibility system. In Sec. 3, we derive the principal equation system in a different and simpler manner from the discrete BGK equation. In Sec. 4, we improve the existing LKS in the efficiency and stability on the basis of the fact that it deals with the artificial compressibility system. Sec. 5 is prepared for the numerical examination of the performance of the original LBM. The LBM, LKS, and the improved LKS are tested in the standing Taylor-Green problem. Appendix A and B report some details regarding the analytical calculations.

2 LBM COMPUTATION BEYOND NAVIER-STOKES

2.1 Asymptotic analysis of isothermal BGK equation

The Boltzmann equation is the basic equation in kinetic theory of gases and describes the time evolution of the distribution function of gas molecules, which is the function of time, space coordinates, and molecular velocity. The fluid-dynamic description of solution of the Boltzmann equation for small Knudsen number is well-known [22, 23]. The Bhatnagar-Gross-Krook (BGK) model equation [24] inherits the main features of the full Boltzmann equation and the fluid-dynamic description solution of BGK solution for small Knudsen numbers is obtained in a much simpler way. Its computational efforts are also much less than the original Boltzmann equation, and therefore, it is quite natural and advantageous to employ the BGK equation as the basis of kinetic method for incompressible Navier-Stokes equation. One of the drawbacks of

the BGK equation is that the recovered Prandtl number is unity while the original Boltzmann equation yields the values nearly to 2/3. Since most of the LBM schemes do not consider the energy equation, the problem of recovering the wrong thermal diffusivity can be omitted. At the same time, as will be seen later, it is allowed to employ the isothermal BGK with a constant collision frequency for this purpose. In this paper, we will follow this path. The reported results can be easily extended for thermal cases as well. This is particularly evident for purely macroscopic FD schemes.

The dimensionless form of the simplified BGK equation is written as

$$\frac{\partial f}{\partial \hat{t}} + v_i \frac{\partial f}{\partial \hat{x}_i} = \lambda \left(f_e - f \right), \tag{1}$$

where $\hat{x}_i$, $\hat{t}$, and v_i are the (dimensionless) space coordinates, time, and molecular velocity components, respectively; f is the distribution function of gas molecules; λ is a positive constant of the order of unit; and finally f_e is the equilibrium distribution function, namely

$$f_e = \hat{\rho} \left(\frac{3}{2\,\pi} \right)^{D/2} \exp \left[-\frac{3(v_i - \hat{u}_i)^2}{2} \right], \tag{2}$$

where

$$\hat{\rho} = \langle\langle f \rangle\rangle, \qquad \hat{q}_i = \hat{\rho}\hat{u}_i = \langle\langle v_i\, f \rangle\rangle, \tag{3}$$

and

$$\langle\langle \cdot \rangle\rangle = \int_{-\infty}^{+\infty} \cdot \, \Pi_{m=1}^{D} dv_m, \tag{4}$$

where D is the number of dimensions. In the following, $D = 2$ is assumed, i.e. the two dimensional case is considered. Recall that the unit of space coordinate and that of time variable in Eq. (1) are the mean free path l_c and the mean collision time T_c, respectively. The ratio $c = l_c/T_c$ is an estimation of the average modulus of the molecule velocity. Obviously, they are not appropriate as the characteristic scales for flow field in the continuum limit. For this reason, in order to make it more evident, all the quantities which are normalized by characteristic scales not appropriate for flow field in the continuum limit are written with a hat $\hat{\cdot}$. Let the characteristic length scale of the flow field be L and let the characteristic flow speed be U. There are two factors in the incompressible continuum limit. The continuum limit means $l_c \ll L$ and the incompressible limit means $U \ll c$. In the following asymptotic analysis, we introduce the other dimensionless variables, defined by

$$x_i = (l_c/L)\hat{x}_i, \qquad t = (UT_c/L)\hat{t}. \tag{5}$$

Defining the small parameter ϵ as $\epsilon = l_c/L$, which corresponds to the Knudsen number, we have $x_i = \epsilon \hat{x}_i$. Furthermore, assuming

$$U/c = \epsilon, \tag{6}$$

which is the key of derivation of the incompressible limit [25, 26], we have $t = \epsilon^2 \hat{t}$. Then, Eq. (1) is rewritten as

$$\epsilon^2 \frac{\partial f}{\partial t} + \epsilon v_i \frac{\partial f}{\partial x_i} = \lambda \left(f_e - f \right), \tag{7}$$

where

$$f(\hat{t}, \hat{x}_i, v_i) = f(t/\epsilon^2, x_i/\epsilon, v_i), \qquad f_e(\hat{t}, \hat{x}_i, v_i) = f_e(t/\epsilon^2, x_i/\epsilon, v_i). \tag{8}$$

In this new scaling, we can assume

$$\frac{\partial f}{\partial \alpha} = O(f), \qquad \frac{\partial \hat{M}}{\partial \alpha} = O(\hat{M}), \tag{9}$$

where $\alpha = t, x_i$ and $\hat{M} = \hat{\rho}, \hat{u}_i, \hat{q}_i$. Actually the previous equations are the rigorous definitions of the characteristic scales for the flow field, L and L/U, or equivalently the definitions of L and U.

The solution of Eq. (7) for small ϵ is investigated in the form of the asymptotic expansion

$$f = f^{(0)} + \epsilon f^{(1)} + \epsilon^2 f^{(2)} + \cdots . \tag{10}$$

$\hat{\rho}$ and $\hat{u}_i$ are also expanded:

$$\hat{\rho} = 1 + \epsilon \rho^{(1)} + \epsilon^2 \rho^{(2)} + \cdots , \tag{11}$$

$$\hat{u}_i = \epsilon u_i^{(1)} + \epsilon^2 u_i^{(2)} + \cdots , \tag{12}$$

and consequently

$$\hat{q}_i = \epsilon q_i^{(1)} + \epsilon^2 q_i^{(2)} + \cdots = \epsilon u_i^{(1)} + \epsilon^2 [u_i^{(2)} + \rho^{(1)} u_i^{(1)}] + \epsilon^3 [u_i^{(3)} + \rho^{(2)} u_i^{(1)} + \rho^{(1)} u_i^{(2)}] \cdots . \tag{13}$$

Since the Mach number is $O(\epsilon)$, the perturbations starts from the order of ϵ. Corresponding to Eq. (9), the coefficients in these expansions are assumed to satisfy

$$\frac{\partial f^{(m)}}{\partial \alpha} = O(1), \qquad \frac{\partial M^{(m)}}{\partial \alpha} = O(1), \tag{14}$$

where $\alpha = t, x_i$ and $M = \rho, u_i, q_i$. Introducing the previous expansions in the Eq. (2), applying Taylor expansion to f_e yields:

$$f_e = f_e^{(0)} + \epsilon f_e^{(1)} + \epsilon^2 f_e^{(2)} + \cdots , \tag{15}$$

where $f_e^{(k)}$ $(k = 1, 2, \cdots)$ are known polynomial functions of the moments.

Substituting the above expansions into Eq. (7) and equating the terms of the same order of power of ϵ, we have

$$0 = \lambda (f_e^{(k)} - f^{(k)}) \qquad (k = 0, 1), \tag{16}$$

$$\frac{\partial f^{(k-2)}}{\partial t} + v_i \frac{\partial f^{(k-1)}}{\partial x_i} = \lambda(f_e^{(k)} - f^{(k)}) \qquad (k \geq 2). \tag{17}$$

In particular Eqs. (17) can be expressed in compact form as

$$f^{(k)} = f_e^{(k)} - \tau \left[\partial_t f^{(k-2)} + \partial_s f^{(k-1)}\right], \tag{18}$$

where $\tau = 1/\lambda$ and the operator ∂_s is

$$\partial_s = v_i \frac{\partial}{\partial x_i}, \tag{19}$$

where the convention of summation is assumed. From the previous relation the full set of coefficients involved in the regular expansion can be recovered, namely

$$f^{(0)} = f_e^{(0)}, \tag{20}$$

$$f^{(1)} = f_e^{(1)}, \tag{21}$$

$$f^{(2)} = f_e^{(2)} - \tau \left[\partial_t f_e^{(0)} + \partial_s f_e^{(1)}\right], \tag{22}$$

$$f^{(3)} = f_e^{(3)} - \tau \left[\partial_t f_e^{(1)} + \partial_s f_e^{(2)}\right] + \tau^2 \left[\partial_t \partial_s f_e^{(0)} + \partial_s^2 f_e^{(1)}\right], \tag{23}$$

$$\begin{aligned} f^{(4)} = {} & f_e^{(4)} - \tau \left[\partial_t f_e^{(2)} + \partial_s f_e^{(3)}\right] + \tau^2 \left[\partial_t^2 f_e^{(0)} + 2\,\partial_t \partial_s f_e^{(1)} + \partial_s^2 f_e^{(2)}\right] \\ & -\tau^3 \left[\partial_t \partial_s^2 f_e^{(0)} + \partial_s^3 f_e^{(1)}\right], \end{aligned} \tag{24}$$

$$\begin{aligned} f^{(5)} = {} & f_e^{(5)} - \tau \left[\partial_t f_e^{(3)} + \partial_s f_e^{(4)}\right] + \tau^2 \left[\partial_t^2 f_e^{(1)} + 2\,\partial_t \partial_s f_e^{(2)} + \partial_s^2 f_e^{(3)}\right] \\ & -\tau^3 \left[2\,\partial_t^2 \partial_s f_e^{(0)} + \partial_t \partial_s^2 f_e^{(1)} + 3\,\partial_s^3 f_e^{(2)}\right] + \tau^4 \left[\partial_t \partial_s^3 f_e^{(0)} + \partial_s^4 f_e^{(1)}\right]. \end{aligned} \tag{25}$$

The above equations give the functional forms of $f^{(k)}$ $(k = 1, 2, \cdots)$ as the functions of the molecular velocity. However, $f^{(k)}$ are not solved with respect to t and x_i. Since $\langle\langle f_e - f \rangle\rangle = \langle\langle v_i(f_e - f)\rangle\rangle = 0$, the left hand sides in Eqs. (17) must satisfy the orthogonality condition

$$\langle\langle \phi(\frac{\partial f^{(k-2)}}{\partial t} + v_i \frac{\partial f^{(k-1)}}{\partial x_i})\rangle\rangle = 0 \qquad (k \geq 2), \tag{26}$$

where $\phi = 1, v_j$, or equivalently, using the compact notation,

$$\langle\langle \phi \left[\partial_t f^{(k-2)} + \partial_s f^{(k-1)}\right]\rangle\rangle = 0 \qquad (k \geq 2). \tag{27}$$

From the above orthogonality conditions, we have the PDE systems for $\rho^{(k)}$ and $u_i^{(k)}$. Once these PDE systems are solved under appropriate boundary

condition and initial data, the asymptotic solution for Eq. (7) is determined. From the orthogonality condition (26) for $k = 2, 3, 4, 5$, we have

$$\frac{\partial q_i^{(1)}}{\partial x_i} = 0, \tag{28}$$

$$\frac{\partial \rho^{(1)}}{\partial x_i} = 0, \tag{29}$$

$$\frac{\partial \rho^{(1)}}{\partial t} + \frac{\partial q_i^{(2)}}{\partial x_i} = \frac{1}{3\lambda}\frac{\partial^2 \rho^{(1)}}{\partial x_k^2}, \tag{30}$$

$$\frac{\partial q_j^{(1)}}{\partial t} + \frac{\partial (q_k^{(1)} q_j^{(1)})}{\partial x_k} + \frac{1}{3}\frac{\partial \rho^{(2)}}{\partial x_j} = \frac{1}{3\lambda}\frac{\partial^2 q_j^{(1)}}{\partial x_k^2}, \tag{31}$$

$$\frac{\partial \rho^{(2)}}{\partial t} + \frac{\partial q_i^{(3)}}{\partial x_i} = \frac{1}{3\lambda}\frac{\partial^2 \rho^{(2)}}{\partial x_k^2} + \frac{1}{\lambda}\frac{\partial^2 (q_i^{(1)} q_j^{(1)})}{\partial x_i \partial x_j}, \tag{32}$$

$$\begin{aligned}\frac{\partial q_j^{(2)}}{\partial t} + \frac{\partial (q_k^{(1)} q_j^{(2)})}{\partial x_k} + \frac{\partial (q_k^{(2)} q_j^{(1)})}{\partial x_k} - \frac{\partial (\rho^{(1)} q_k^{(1)} q_j^{(1)})}{\partial x_k} + \frac{1}{3}\frac{\partial \rho^{(3)}}{\partial x_j} = \frac{1}{3\lambda}\frac{\partial^2 q_j^{(2)}}{\partial x_k^2} \\ + \frac{2}{3\lambda}\frac{\partial^2 q_k^{(2)}}{\partial x_j \partial x_k} + \frac{2}{3\lambda}\frac{\partial^2 \rho^{(1)}}{\partial t \partial x_j} - \frac{1}{3\lambda^2}\frac{\partial^3 \rho^{(1)}}{\partial x_k^2 \partial x_j},\end{aligned} \tag{33}$$

$$\frac{\partial q_i^{(4)}}{\partial x_i} = 0, \tag{34}$$

$$\frac{\partial q_i^{(3)}}{\partial t} + \frac{\partial}{\partial x_j}(u_i^{(1)} q_j^{(3)} + q_i^{(3)} u_j^{(1)}) + \frac{\partial p^{(4)}}{\partial x_i} = \frac{1}{3\lambda}\frac{\partial^2 q_i^{(3)}}{\partial x_k^2} + \frac{1}{3\lambda}\frac{\partial^2 q_j^{(3)}}{\partial x_i \partial x_j} + i_3, \tag{35}$$

where i_3 is a proper term which depends on the lower order coefficients only (see Appendix A for details).

Since the density is expanded around the constant value 1, then $q_i^{(1)} = u_i^{(1)}$, as reported in Eqs. (11, 12, 13). Hence from Eqs. (28) and (31), we have the incompressible NS system of equations

$$\frac{\partial u_i^{(1)}}{\partial x_i} = 0, \tag{36}$$

$$\frac{\partial u_j^{(1)}}{\partial t} + u_i^{(1)}\frac{\partial u_j^{(1)}}{\partial x_i} + \frac{\partial p^{(2)}}{\partial x_j} = \frac{1}{3\lambda}\frac{\partial^2 u_j^{(1)}}{\partial x_k^2}, \tag{37}$$

where $p^{(k)} = \rho^{(k)}/3$. Thus the incompressible NS system of equations, Eqs. (36) and (37), are derived from the continuous simplified BGK equation under the diffusion scaling. From Eq. (29), we get that the leading density field is

uniform, i.e. $\rho^{(1)} = \rho^{(1)}(t)$. In particular, from Eq. (30) we have

$$\frac{\partial q_i^{(2)}}{\partial x_i} = -\frac{d\rho^{(1)}}{dt}. \tag{38}$$

In various situation, such as the problem in a closed domain, where the total mass in the domain is constant, we can naturally assume (or choose) $\rho^{(1)} = 0$. Hence $q_i^{(2)} = u_i^{(2)}$ and we have the solenoidal condition for $u_i^{(2)}$:

$$\frac{\partial u_i^{(2)}}{\partial x_i} = 0. \tag{39}$$

Taking into account the previous simplifications, Eq. (33) yields

$$\frac{\partial u_j^{(2)}}{\partial t} + u_k^{(1)}\frac{\partial u_j^{(2)}}{\partial x_k} + u_k^{(2)}\frac{\partial u_j^{(1)}}{\partial x_k} + \frac{\partial p^{(3)}}{\partial x_i} = \frac{1}{3\lambda}\frac{\partial^2 u_j^{(2)}}{\partial x_k^2}. \tag{40}$$

Eqs. (39) and (40) constitute the homogeneous Oseen system and its solution from homogeneous initial data and boundary condition is zero. Thus, we have

$$\rho^{(3)} = p^{(3)} = 0, \qquad u_i^{(2)} = 0. \tag{41}$$

Taking into account the previous simplifications, Eq. (32) yields

$$\frac{\partial \rho^{(2)}}{\partial t} + \frac{\partial q_i^{(3)}}{\partial x_i} = \frac{1}{\lambda}\left[\frac{\partial^2 p^{(2)}}{\partial x_k^2} + \frac{\partial^2 (u_i^{(1)} u_j^{(1)})}{\partial x_i \partial x_j}\right] = 0. \tag{42}$$

In particular, the previous simplification was achieved by recalling the Poisson equation for the ICNS system of equations.

Eqs. (42) and (35) can be combined in order to produce an additional equation for computing $p^{(4)}$ as a function of $q_i^{(3)}$ (analogously to Poisson equation for the ICNS system of equations). This means that Eqs. (42) and (35) represent the first kinetic effect beyond the ICNS description of the flow, which is not null in general. Clearly any numerical scheme aiming to catch the kinetic effects prescribed by the original physical model, must be consistent with these equations.

Remark 1. Actually it is possible to derive the same leading equations (36-37) and (39-40) for the expansion coefficients by applying the same diffusion scaling to the following macroscopic system

$$\beta\frac{\partial \hat{\rho}}{\partial \hat{t}} + \frac{\partial \hat{u}_i}{\partial \hat{x}_i} = 0, \tag{43}$$

$$\frac{\partial \hat{u}_j}{\partial \hat{t}} + \hat{u}_i\frac{\partial \hat{u}_j}{\partial \hat{x}_i} + \frac{\partial \hat{p}}{\partial \hat{x}_j} = \frac{1}{3\lambda}\frac{\partial^2 \hat{u}_j}{\partial \hat{x}_k^2}. \tag{44}$$

This remark will be discussed again in the following.

In the next Section, these macroscopic equations will be compared with those recovered by a simple LBM scheme.

2.2 Asymptotic analysis of isothermal lattice BGK equation

The key starting point of any numerical scheme based on the lattice Boltzmann method is to consider a finite set of microscopic velocities, called lattice. The LBM simulates the time evolution of a weakly compressible gas flow in nearly continuum regime by solving a kinetic equation on the lattice and yields the solution of the incompressible Navier-Stokes equation as its leading order. As previously stated, LBM does not need to give the accurate behavior of rarefied gas flows. Further, because of computation cost, a simplified kinetic equation, such as the discrete velocity model of isothermal BGK equation with constant collision frequency is often employed as its theoretical basis.

The dimensionless form of the discrete velocity model of the simplified BGK equation is written as

$$\frac{\partial F}{\partial \hat{t}} + V_i \frac{\partial F}{\partial \hat{x}_i} = \lambda \left(F_e - F \right), \tag{45}$$

where V_i is the dimensionless molecular velocity on the lattice, i.e. V_i belongs to a set of Q permitted velocities, F and F_e are lists with Q elements and their elements are functions of $\hat{t}$ and $\hat{x}_i$. In the above dimensionless equation, the time, space coordinate, and molecular velocity are nondimensionalized as described for the original physical model. Moreover λ, which will be employed as a tuning parameter of LBM, is regarded as a constant of the order of unity. In D2Q9 model, the molecular velocity V_i has the following 9 values:

$$V_1 = \begin{bmatrix} 0 & 1 & 0 & -1 & 0 & 1 & -1 & -1 & 1 \end{bmatrix}^T, \tag{46}$$

$$V_2 = \begin{bmatrix} 0 & 0 & 1 & 0 & -1 & 1 & 1 & -1 & -1 \end{bmatrix}^T. \tag{47}$$

Consequently the components of the molecular velocity V_1, V_2, the discrete distribution function F and the discrete equilibrium distribution F_e are all lists with 9 elements.

Before proceeding to the definition of the local equilibrium function F_e, we define the rule of computation for the list. Let H and G be the lists defined by $H = [H_0, H_1, H_2, \cdots, H_8]^T$ and $G = [G_0, G_1, G_2, \cdots, G_8]^T$. Then, HG is the list defined by $[H_0G_0, H_1G_1, H_2G_2, \cdots, H_8G_8]^T$. The sum of all the elements of the list H is denoted by $\langle H \rangle$, i.e. $\langle H \rangle = \sum_{i=0}^{8} H_i$. Then, the dimensionless

density $\hat{\rho}$ and flow velocity $\hat{u}_i$ are defined by

$$\hat{\rho} = \langle F \rangle, \qquad \hat{u}_i = \langle V_i F \rangle. \tag{48}$$

According to Ref. [27], F_e is defined by

$$F_e = \begin{bmatrix} 4/9\,\hat{\rho} - 2/3\,\hat{u}_1^2 - 2/3\,\hat{u}_2^2, \\ 1/9\,\hat{\rho} + 1/3\,\hat{u}_1 + 1/3\,\hat{u}_1^2 - 1/6\,\hat{u}_2^2, \\ 1/9\,\hat{\rho} + 1/3\,\hat{u}_2 + 1/3\,\hat{u}_2^2 - 1/6\,\hat{u}_1^2, \\ 1/9\,\hat{\rho} - 1/3\,\hat{u}_1 + 1/3\,\hat{u}_1^2 - 1/6\,\hat{u}_2^2, \\ 1/9\,\hat{\rho} - 1/3\,\hat{u}_2 + 1/3\,\hat{u}_2^2 - 1/6\,\hat{u}_1^2, \\ 1/36\,\hat{\rho} + 1/12\,(\hat{u}_1 + \hat{u}_2) + 1/8\,(\hat{u}_1 + \hat{u}_2)^2 - 1/24\,(\hat{u}_1^2 + \hat{u}_2^2), \\ 1/36\,\hat{\rho} - 1/12\,(\hat{u}_1 - \hat{u}_2) + 1/8\,(-\hat{u}_1 + \hat{u}_2)^2 - 1/24\,(\hat{u}_1^2 + \hat{u}_2^2), \\ 1/36\,\hat{\rho} - 1/12\,(\hat{u}_1 + \hat{u}_2) + 1/8\,(-\hat{u}_1 - \hat{u}_2)^2 - 1/24\,(\hat{u}_1^2 + \hat{u}_2^2), \\ 1/36\,\hat{\rho} + 1/12\,(\hat{u}_1 - \hat{u}_2) + 1/8\,(\hat{u}_1 - \hat{u}_2)^2 - 1/24\,(\hat{u}_1^2 + \hat{u}_2^2) \end{bmatrix}, \tag{49}$$

where $\hat{p} = \hat{\rho}/3$. $\hat{\rho}$, $\hat{u}_1$ and $\hat{u}_2$ are also obtained as the moments of F_e:

$$\hat{\rho} = \langle F_e \rangle, \qquad \hat{u}_i = \langle V_i F_e \rangle. \tag{50}$$

The discrete equilibrium can be designed by prescribing that 9 linearly independent discrete moments of F_e are equal to the corresponding continuous counterparts. In order to recover Navier-Stokes on the D2Q9 lattice, 8 moments are required (instead of the theoretical 10 because of lattice deficiencies). Hence only one discrete moment is left as "freely" tunable. Historically an even forth-order moment is selected for mimicking the continuous counterpart.

According to Ref. [21], we summarize some convenient formulas related to F_e, which make the analysis of LBM drastically simple. We introduce the operators defined by

$$L_1(F) = \hat{\rho} F^*, \tag{51}$$

$$L_2(F) = 3 V_i \hat{u}_i F^*, \tag{52}$$

$$B(F, G) = \frac{9}{4}(\hat{u}_i \hat{\omega}_j + \hat{u}_j \hat{\omega}_i)(V_i V_j - \frac{1}{3}\delta_{ij}) F^*, \tag{53}$$

where

$$\hat{\rho} = \langle F \rangle, \qquad \hat{u}_i = \langle V_i F \rangle, \qquad \hat{\omega}_i = \langle V_i G \rangle, \tag{54}$$

$$F^* = \frac{1}{36} \begin{bmatrix} 16 & 4 & 4 & 4 & 4 & 1 & 1 & 1 & 1 \end{bmatrix}^T. \tag{55}$$

Then, F_e is expressed as

$$F_e = L_1(F) + L_2(F) + B(F, F). \tag{56}$$

As for the moments of F^*, the following relations hold:

$$\begin{aligned} \langle F^* \rangle = 1, \qquad \langle V_i V_j F^* \rangle = \frac{1}{3}\delta_{ij}, \\ \langle V_i V_j V_k V_l \rangle = \frac{1}{9}(\delta_{ij}\delta_{kl} + \delta_{ik}\delta_{jl} + \delta_{il}\delta_{jk}), \\ \langle V_i F^* \rangle = \langle V_i V_j V_k F^* \rangle = \langle V_i V_j V_k V_l V_m F^* \rangle = 0, \end{aligned} \tag{57}$$

from which we have

$$\begin{aligned} \langle L_1(F) \rangle = \hat{\rho}, \qquad \langle L_2(F) \rangle = 0, \qquad \langle B(F, G) \rangle = 0, \\ \langle V_i L_1(F) \rangle = 0, \qquad \langle V_i L_2(F) \rangle = \hat{u}_i, \qquad \langle V_i B(F, G) \rangle = 0, \\ \langle V_i V_j L_1(F) \rangle = \frac{1}{3}\hat{\rho}\delta_{ij}, \qquad \langle V_i V_j L_2(F) \rangle = 0, \\ \langle V_i V_j B(F, G) \rangle = \frac{1}{2}(\hat{u}_i\hat{\omega}_j + \hat{u}_j\hat{\omega}_i), \end{aligned} \tag{58}$$

and so on.

In order to avoid any interpolation, the velocity lattice is used to generate a homogeneous spatial mesh. The coordinates of spatial discrete points employed in the LBM computation are $(\hat{x}, \hat{y}) = (l, m)$, where l and m are integers. Let $\hat{x}_i^P$ be the coordinate of a lattice point. Then, $\hat{x}_i^P - V_i^{(k)}$ is the coordinate of a lattice adjacent to the lattice point $\hat{x}_i^P$. LBM computation is nothing more than the forward Euler time integration formula of Eq. (45) with the time step of the unity:

$$F(\hat{t} + 1, \hat{x}_i, V_i) = F(\hat{t}, \hat{x}_i - V_i, V_i) + \lambda\, G(\hat{t}, \hat{x}_i - V_i, V_i), \tag{59}$$

where

$$G = F_e - F. \tag{60}$$

Recall that the unit of space coordinate and that of time variable in Eq. (59) are the mean free path $l_c (= cT_c)$ and the mean collision time T_c, respectively. As already pointed out for the continuous case, they are not appropriate as the characteristic scales for flow field in the continuum limit. The same asymptotic analysis for the continuous case can be repeated for the system of equations referring to the considered lattice. Introducing a proper scaling [25, 26] in Eq.(59), i.e. assuming $\hat{t} = t/\epsilon^2$ and $\hat{x}_i = x_i/\epsilon$, yields

$$F(t + \epsilon^2, x_i, V_i) = F(t, x_i - V_i\epsilon, V_i) + \lambda\, G(t, x_i - V_i\epsilon, V_i). \tag{61}$$

We express $F(t+\epsilon^2, x_i, V_i)$, $F(t, x_i - V_i\epsilon, V_i)$, and $G(t, x_i - V_i\epsilon, V_i)$ as their Taylor expansions around (t, x_i)

$$F(t+\epsilon^2, x_i, V_i) = \sum_{k=0}^{\infty} \frac{\epsilon^{2k}}{k!} \left(\frac{\partial}{\partial t}\right)^k F(t, x_i, V_i), \tag{62}$$

$$F(t, x_i - V_i\epsilon, V_i) = \sum_{k=0}^{\infty} \frac{(-\epsilon)^k}{k!} D^k F(t, x_i, V_i), \tag{63}$$

$$G(t, x_i - V_i\epsilon, V_i) = \sum_{k=0}^{\infty} \frac{(-\epsilon)^k}{k!} D^k G(t, x_i, V_i), \tag{64}$$

where $\dot{\partial}_S = V_1\dot{\partial}_x + V_2\dot{\partial}_y$.

Similar to the asymptotic analysis for the discrete velocity BGK equation, we assume f in the form

$$F = F^* + \epsilon F^{(1)} + \epsilon^2 F^{(2)} + \cdots . \tag{65}$$

Corresponding to the expansion, f_e is expressed in the form:

$$F_e = F^* + \epsilon F_e^{(1)} + \epsilon^2 F_e^{(2)} + \cdots , \tag{66}$$

$$G = \epsilon G^{(1)} + \epsilon^2 G^{(2)} + \cdots , \tag{67}$$

where

$$F_e^{(1)} = L_1(F^{(1)}) + L_2(F^{(1)}), \tag{68}$$

$$F_e^{(k)} = L_1(F^{(k)}) + L_2(F^{(k)}) + \sum_{\substack{a+b=k \\ a\geq 1, b\geq 1}} B(F^{(a)}, F^{(b)}) \qquad (k \geq 2), \tag{69}$$

$$G^{(k)} = F_e^{(k)} - F^{(k)}. \tag{70}$$

Substituting the above expansions into Eq. (61) and equating the terms of the same order of power of ϵ, we derive the expressions for the distribution function coefficients $F^{(k)}$ $(k = 1, 2, \cdots)$, namely

$$F^{(k)} = F_e^{(k)} - G^{(k)}, \tag{71}$$

$$G^{(1)} = 0, \tag{72}$$

$$G^{(2)} = \tau \partial_S F_e^{(1)}, \tag{73}$$

$$G^{(3)} = \tau[\partial_t F_e^{(1)} + \partial_S F_e^{(2)} - \omega_1 \partial_S^2 F_e^{(1)}], \tag{74}$$

$$G^{(4)} = \tau[\partial_t F_e^{(2)} + \partial_S F_e^{(3)} - \omega_1(\partial_S^2 F_e^{(2)} + 2\,\partial_S \partial_t F_e^{(1)}) + \omega_2 \partial_S^3 F_e^{(1)}], \tag{75}$$

$$\begin{aligned} G^{(5)} =& \tau[\partial_t F_e^{(3)} + \partial_S F_e^{(4)} - \omega_1(\partial_t^2 F_e^{(1)} + 2\,\partial_S \partial_t F_e^{(2)} + \partial_S^2 F_e^{(3)}) \\ &+ \omega_2(\partial_S^3 F_e^{(2)} + 3\,\partial_S^2 \partial_t F_e^{(1)}) - \omega_3 \partial_S^4 F_e^{(1)}], \end{aligned} \tag{76}$$

where

$$\omega_1 = \tau - 1/2, \tag{77}$$

$$\omega_2 = \tau^2 - \tau + 1/6, \tag{78}$$

$$\omega_3 = \tau^3 - 3/2\,\tau^2 + 7/12\,\tau - 1/24. \tag{79}$$

Clearly the discrete effects due to the low accuracy of the forward Euler integration rule is shown by the fact that $\omega_1 \neq \tau$, $\omega_2 \neq \tau^2$ and $\omega_3 \neq \tau^3$, as it should be for the continuous model: this is evident by comparing the previous equations with Eqs. (20-25).

From the orthogonality conditions $\langle G^{(m)} \rangle = 0$ and $\langle V_k G^{(m)} \rangle = 0$, we have the PDE systems for $p^{(m)}$ and $u_k^{(m)}$, which are summarized as follows.

$$\frac{\partial u_i^{(1)}}{\partial x_i} = 0, \tag{80}$$

$$\frac{\partial u_j^{(1)}}{\partial t} + \frac{\partial (u_i^{(1)} u_j^{(1)})}{\partial x_i} + \frac{\partial p^{(2)}}{\partial x_i} = \frac{\omega_1}{3} \frac{\partial^2 u_j^{(1)}}{\partial x_k^2}, \tag{81}$$

$$\frac{\partial u_i^{(2)}}{\partial x_i} = 0. \tag{82}$$

$$\frac{\partial u_j^{(2)}}{\partial t} + \frac{\partial (u_i^{(1)} u_j^{(2)} + u_i^{(2)} u_j^{(1)})}{\partial x_i} + \frac{\partial p^{(3)}}{\partial x_i} = \frac{\omega_1}{3} \frac{\partial^2 u_j^{(2)}}{\partial x_k^2}, \tag{83}$$

$$\frac{\partial \rho^{(2)}}{\partial t} + \frac{\partial q_i^{(3)}}{\partial x_i} = 0. \tag{84}$$

$$\frac{\partial q_i^{(3)}}{\partial t} + \frac{\partial}{\partial x_j}(u_i^{(1)} q_j^{(3)} + q_i^{(3)} u_j^{(1)}) + \frac{\partial p^{(4)}}{\partial x_i} = \frac{\omega_1}{3} \frac{\partial^2 q_i^{(3)}}{\partial x_k^2} + \frac{\omega_1}{3} \frac{\partial^2 q_j^{(3)}}{\partial x_i \partial x_j} + I_3, \tag{85}$$

where the inhomogeneous term I_3 consists of the lower moments and its derivatives [1] (see Appendix B for details).

[1] The adopted definition of discrete equilibrium (49) is based on the so-called incompressible approximation [27], i.e. the fact that density effects are neglected in higher order moments. Because of these approximation, $q_i^{(3)} = u_i^{(3)}$ for the simple LBM scheme. In the previous formulas, the notation $q_i^{(3)}$ has been adopted in order to simplify the comparison between the LBM case given by Eq. (85) and the continuous case given by Eq. (35).

Remark 2. Summing up Eqs. (80, 82, 84) and Eqs. (81, 83, 85) yields respectively

$$\epsilon^2 \frac{\partial \bar{\rho}}{\partial t} + \frac{\partial \bar{u}_i}{\partial x_i} = 0, \tag{86}$$

$$\frac{\partial \bar{u}_i}{\partial t} + \bar{u}_j \frac{\partial \bar{u}_i}{\partial x_j} + \frac{\partial \bar{p}}{\partial x_i} = \frac{\omega_1}{3} \frac{\partial^2 \bar{u}_i}{\partial x_j^2}. \tag{87}$$

where $\bar{\rho} = (\hat{\rho} - 1)/\epsilon^2$ and $\bar{u}_i = \hat{u}_i/\epsilon$. Clearly the previous system traces the Chorin's ACM with mesh dependent parameter. The solution of the previous system approximates the incompressible NS equation with viscosity $\omega_1/3 = (1/3)(1/\lambda - 1/2)$ and error of $O(\epsilon^2)$.

Let us compare the equations recovered by the simple LBM scheme with those for the original physical model.

- First of all, the actual transport coefficients ω_i prescribed by the numerical scheme are not the same of the original kinetic model. This problem may be partially fixed by changing the definitions of the transport coefficients.
- The second problem is that the truncated local equilibrium is not enough to describe some of the terms appearing in the equations ruling the dynamics of the higher order moments. This problem may be fixed by considering a more accurate approximation of the local equilibrium, in terms of polynomial forms.
- Finally, since only few discrete velocities are considered by the simple LBM scheme, some spurious terms appear in the differential operators ruling the dynamics of the higher order moments. For example, the D2Q9 lattice is not enough accurate to catch the physics up to the Burnett-like order, i.e. the set of equations ruling the deviations from the ICNS description. As a proof, see the difference between forcing term i_3 reported in Appendix A for the original kinetic model and I_3 reported in Appendix B derived by the simple LBM scheme.

Hence, if special treatments are not considered, and, in particular, larger lattices are not used or proper corrective terms are designed, it is impossible to claim that the simple LBM scheme may naturally catch physics beyond the NS description of the flow. The present study indeed moderates the expectations on the fact that "standard" LBM schemes can realize a slip theory for micro-flows [28, 29, 30, 31], although it does not prevent the improvement of the NS system by replacing the nonslip boundary condition with the slip boundary condition. In particular, it is worth the effort to point out that, even though LBM is formulated in terms of the particle distribution function, this does not ensure one to naturally catch the flow dependence on Knudsen number, including the slip velocity, despite some of these claims are sometimes reported in literature [28]. This misunderstanding has been already pointed out [32]. Hence the so-called kinetic content of LBM should be addressed more carefully.

LBM deals with a complete kinetic description of the flow, even though the numerical accuracy is tuned in such a way to recover only the Navier-Stokes equations and this leads to "non-existing" higher order rarefaction effect. For higher order rarefaction effect, we intend the macroscopic fluid dynamics beyond Navier-Stokes system of equations. This fake rarefaction effect becomes more real, only when the stencil becomes larger. If we want to deal with physically correct kinetic effect beyond Navier-Stokes, we should use non-isothermal BGK equation at least. Even in the simple framework of isothermal BGK, the LBM with usual stencil cannot deal with physically relevant kinetic effect beyond Navier-Stokes.

3 TRUNCATED MOMENT SYSTEM

In the previous section, we compare the equations solved at macroscopic level by LBM with those prescribed by the original kinetic model up to the Burnett-like order. We found that as far as we proceed beyond Navier-Stokes with the simple D2Q9 lattice, some differences between LBM and the kinetic model arise, which can not be filled by elementary tricks. Although the applied asymptotic analysis [21] is effective, however, it sometimes considered a bit complicated. Hence a simpler strategy is suggested in this section, in order to derive the equivalent macroscopic system. Instead of going through the asymptotic analysis, we can directly derive the artificial compressibility system. We already realized that the simple forward Euler integration rule forces one to redefine the macroscopic transport coefficients, because of the discrete error effects. This induces us to introduce the coefficients ω_i. In order to avoid this eventuality, the discrete velocity model defined by Eq. (45) will be adopted instead of LBM updating rule as starting point.

Let us introduce the diffusion scaling [25, 26] in Eq. (45). Recalling the essential steps reported in the previous Section 2, defining the small parameter ϵ as $\epsilon = l_c/L$, which corresponds to the Knudsen number, we have $x_i = \epsilon \hat{x}_i$. Furthermore assuming $U/c = \epsilon$, we have $t = \epsilon^2 \hat{t}$. Finally Eq. (45) becomes

$$\epsilon^2 \frac{\partial F}{\partial t} + \epsilon V_i \frac{\partial F}{\partial x_i} = \lambda \left(F_e - F \right). \tag{88}$$

Let us introduce the general nomenclature for non-conserved equilibrium moments

$$\Pi^e_{\overbrace{11\cdots1}^{n \text{ times}}\,\overbrace{22\cdots2}^{m \text{ times}}} = \langle V_1^n V_2^m F_e \rangle. \tag{89}$$

The previous nomenclature can be expressed for non-conserved generic mo-

ments as well, namely

$$\Pi_{11\cdots1\,22\cdots2}(\overbrace{11\cdots1}^{n\text{ times}},\overbrace{22\cdots2}^{m\text{ times}}) = \langle V_1^n V_2^m F\rangle. \tag{90}$$

Let us define a matrix $M = [1;\, V_1;\, V_2;\, V_1^2;\, V_2^2;\, V_1V_2;\, V_1(V_2)^2;\, (V_1)^2V_2;\, (V_1)^2(V_2)^2]^T$, which involves proper combinations of the lattice velocity components. For example, the matrix M can be used to compute some equilibrium moments, namely

$$MF_e = \begin{bmatrix} \hat{\rho} \\ \hat{q}_1 \\ \hat{q}_2 \\ \Pi^e_{11} \\ \Pi^e_{22} \\ \Pi^e_{12} \\ \Pi^e_{221} \\ \Pi^e_{112} \\ \Pi^e_{1122} \end{bmatrix} = \begin{bmatrix} \hat{\rho} \\ \epsilon\, u_1 \\ \epsilon\, u_2 \\ \hat{p} + \epsilon^2\, u_1^2 \\ \hat{p} + \epsilon^2\, u_2^2 \\ \epsilon^2\, u_1 u_2 \\ \epsilon\, u_1/3 \\ \epsilon\, u_2/3 \\ \hat{p}/3 + \epsilon^2\, u_1^2/3 + \epsilon^2\, u_2^2/3 \end{bmatrix}, \tag{91}$$

where $\hat{p} = \hat{\rho}/3$ and $\hat{u}_i = \epsilon\, u_i$, because of the low Mach number limit.

Property 1. In particular for the considered D2Q9, the following equivalences hold

$$V_1V_1V_1 = V_1 \qquad V_2V_2V_2 = V_2. \tag{92}$$

For example, taking into account the previous equivalences, it is immediate to realize that $\Pi_{111} = \Pi_1 = \epsilon u_1$ and $\Pi_{222} = \Pi_2 = \epsilon u_2$.

Property 2. Since the adopted diffusion scaling assumes that the system is close to the local equilibrium, the following properties hold

$$\Pi_{11\cdots1\,22\cdots2} = O(\Pi^e_{11\cdots1\,22\cdots2}), \qquad \frac{\partial \Pi_{11\cdots1\,22\cdots2}}{\partial \alpha} = O\left(\frac{\partial \Pi^e_{11\cdots1\,22\cdots2}}{\partial \alpha}\right), \tag{93}$$

where $\alpha = t, x_i$. Property 2 is not an assumption, but a simple consequence of our searching of the continuum regime in the limiting case of small Knudsen number. Whatever (diffusion or acoustic) scaling we adopt, the leading term ruling the dynamics of any moment, in the limiting case of small Knudsen number, will always be the corresponding equilibrium part.

We can now apply the asymptotic analysis of the LBM scheme based on the Grad moment system. Let us compute the first moments of the Eq. (88)

(corresponding to the first three rows of the matrix M), namely

$$\frac{\partial \hat{\rho}}{\partial t} + \frac{\partial u_i}{\partial x_i} = 0, \tag{94}$$

$$\epsilon^3 \frac{\partial u_i}{\partial t} + \epsilon \frac{\partial \Pi_{i\,j}}{\partial x_j} = 0. \tag{95}$$

In the momentum equation, the generic expression of the stress tensor appears. The components of the stress tensor satisfy the following equations

$$\epsilon^2 \frac{\partial \Pi_{11}}{\partial t} + \epsilon^2 \frac{\partial u_1}{\partial x_1} + \epsilon \frac{\partial \Pi_{112}}{\partial x_2} = \lambda \left(\hat{p} + \epsilon^2 u_1^2 - \Pi_{11} \right), \tag{96}$$

$$\epsilon^2 \frac{\partial \Pi_{22}}{\partial t} + \epsilon \frac{\partial \Pi_{221}}{\partial x_1} + \epsilon^2 \frac{\partial u_2}{\partial x_2} = \lambda \left(\hat{p} + \epsilon^2 u_2^2 - \Pi_{22} \right), \tag{97}$$

$$\epsilon^2 \frac{\partial \Pi_{12}}{\partial t} + \epsilon \frac{\partial \Pi_{112}}{\partial x_1} + \epsilon \frac{\partial \Pi_{221}}{\partial x_2} = \lambda \left(\epsilon^2 u_1 u_2 - \Pi_{12} \right), \tag{98}$$

where both equivalences given by Eq. (92) and the the commutative property of multiplication were used. In the previous equations, the new unknowns Π_{112} and Π_{221} appear. The equations ruling these two moments are

$$\epsilon^2 \frac{\partial \Pi_{112}}{\partial t} + \epsilon \frac{\partial \Pi_{12}}{\partial x_1} + \epsilon \frac{\partial \Pi_{1122}}{\partial x_2} = \lambda \left(\epsilon\, u_2/3 - \Pi_{112} \right), \tag{99}$$

$$\epsilon^2 \frac{\partial \Pi_{221}}{\partial t} + \epsilon \frac{\partial \Pi_{1122}}{\partial x_1} + \epsilon \frac{\partial \Pi_{12}}{\partial x_2} = \lambda \left(\epsilon\, u_1/3 - \Pi_{221} \right), \tag{100}$$

where the new unknown Π_{1122} appears. Finally the latter moment satisfies

$$\epsilon^2 \frac{\partial \Pi_{1122}}{\partial t} + \epsilon \frac{\partial \Pi_{221}}{\partial x_1} + \epsilon \frac{\partial \Pi_{112}}{\partial x_2} = \lambda \left(\hat{p}/3 + \epsilon^2\, u_1^2/3 + \epsilon^2\, u_2^2/3 - \Pi_{1122} \right), \tag{101}$$

where no new unknowns appear. This clearly means that at this point the sequence of equations ruling the discrete moments is automatically truncated. The assumption to consider a lattice, i.e. a finite set of Q discrete velocities, is enough to produce a closure in the moment system. In particular, only Q independent moment equations exist.

From Eq. (95) and taking into account the property given by Eq. (93)

$$\frac{\partial \Pi_{i\,j}}{\partial x_j} = O\left(\frac{\partial \hat{p}}{\partial x_i} \right) = O(\epsilon^2). \tag{102}$$

Consequently, in various situations, such as the problem in a closed domain, where the total mass in the domain is constant, we can naturally assume $\hat{p} = p_0 + \epsilon^2 p$, where p_0 is a constant, or equivalently $\hat{\rho} = \rho_0 + \epsilon^2 \rho$, where ρ_0 is another constant. Introducing the previous expression in Eq. (94) yields

$$\frac{\partial u_i}{\partial x_i} = -\epsilon^2 \frac{\partial \rho}{\partial t}, \tag{103}$$

which means that the recovered velocity field is divergence-free, as far as the terms $O(\epsilon^2)$ are neglected.

Taking into account the property given by Eq. (93)

$$\frac{\partial \Pi_{ij\,k}}{\partial x_k} = O(\epsilon). \tag{104}$$

From Eq. (102) and taking into account the property given by Eq. (93)

$$\frac{\partial \Pi_{ijk\,l}}{\partial x_l} = O(\epsilon^2). \tag{105}$$

Collecting the previous results, Eqs. (102-105, 99) yield $\Pi_{112} = \epsilon\, u_2/3 + O(\epsilon^3)$, while Eqs. (102-105, 100) yield $\Pi_{221} = \epsilon\, u_1/3 + O(\epsilon^3)$. Introducing these expressions in Eqs. (96-98) yield

$$O(\epsilon^4) + \epsilon^2 \frac{\partial u_1}{\partial x_1} + \epsilon^2 \frac{1}{3}\frac{\partial u_2}{\partial x_2} = \lambda \left(p_0 + \epsilon^2 p + \epsilon^2 u_1^2 - \Pi_{11} \right), \tag{106}$$

$$O(\epsilon^4) + \epsilon^2 \frac{1}{3}\frac{\partial u_1}{\partial x_1} + \epsilon^2 \frac{\partial u_2}{\partial x_2} = \lambda \left(p_0 + \epsilon^2 p + \epsilon^2 u_2^2 - \Pi_{22} \right), \tag{107}$$

$$O(\epsilon^4) + \epsilon^2 \frac{1}{3}\frac{\partial u_2}{\partial x_1} + \epsilon^2 \frac{1}{3}\frac{\partial u_1}{\partial x_2} = \lambda \left(\epsilon^2 u_1 u_2 - \Pi_{12} \right), \tag{108}$$

or equivalently, taking into account Eq. (103),

$$\Pi_{ij} = (p_0 + \epsilon^2 p)\, \delta_{ij} + \epsilon^2 u_i u_j - \frac{\epsilon^2}{3\lambda} \left(\frac{\partial u_i}{\partial x_j} + \frac{\partial u_j}{\partial x_i} \right) + O(\epsilon^4). \tag{109}$$

Finally, introducing Eq. (109) into Eq. (95) and taking into account Eq. (103) yields

$$\frac{\partial u_i}{\partial t} + u_j \frac{\partial u_i}{\partial x_j} + \frac{\partial p}{\partial x_i} = \nu \frac{\partial^2 u_i}{\partial x_j^2} + O(\epsilon^2), \tag{110}$$

where $\nu = 1/(3\,\lambda)$. Clearly Eqs. (103, 110) approximate the NS system of equations, if errors $\sim O(\epsilon^2)$ are neglected.

Over twenty five years ago, Chorin [15] proposed a computationally efficient method for computing viscous incompressible flow in steady state conditions by means of artificial compressibility. Obviously the LBM method shares some features with the Chorin's method, as proved by Eqs. (103, 110). However the LBM is usually considered a good solver for transient flows too, if proper scaling of the quantities can be assumed. The reason is that the artificial compressibility $\epsilon^2\, \partial_t \rho$ in Eq. (103) is not only negligible but also grid depending. In this way, the grid size is introduced as a perturbation parameter in the

system of equations and this leads to solutions depending on it according to the diffusion scaling.

Remark 3. Neglecting terms $\sim O(\epsilon^2)$ in Eq. (110) and considering the obtained equation together with Eq. (103) yields a system which is perfectly equivalent to Eqs. (86, 87), since it is evident, from the previous definitions, that $\bar{\rho} \equiv \rho$ and $\bar{u}_i \equiv u_i$. Taking into account the diffusion scaling, this system is equivalent as well with Eqs. (43, 44), if $\beta = 1$ is assumed. Moreover this remark will be recalled in deriving a simple ACM scheme in Section 5.

Some final comments are reported.

- The asymptotic expansions for the fluid dynamic conserved moments are neither that considered by the Chapman-Enskog procedure (which expands the distribution function and moment equations but it does not expand the macroscopic variables) nor the Hilbert procedure (which expands both the distribution function and the macroscopic variables, and consequently, moment equations).
- The proposed expansion based on the truncated moment system is definitively easier than that based on the Hilbert expansion. Maybe in the case of the simple fluid, the difference is not so evident. However applying the Hilbert expansion in case of multi-relaxation-time models and, for example, in case of multi-components is a different matter [33]. In these cases, the proposed procedure is much simpler and equally effective.
- The proposed asymptotic analysis immediately allows one to appreciate the hierarchy of macroscopic moment equations and consequently to understand which term must be modified, in order to design new scheme for solving modified equations. In particular the order of the higher moments involved in the dynamics of a given moment is immediately evident.

In this section, it has been proved that the key point in the derivation of the macroscopic equations is the diffusion scaling and that complex expansions of the hydrodynamic conserved moments can be avoided.

4 IMPROVED LKS: FD-LKSν

It is pointed out in Sections 2 that the macroscopic equations recovered from LBM by means of the systematic asymptotic analysis differ from those obtained from the continuous BGK equation at the Burnett level. The principal macroscopic equation system, which is common for both cases and derives Chorin's ACM, is also obtained from the moment analysis of the discrete BGK equation (Sec. 3). It is seen from these discussions that the kinetic formulation for the low Mach number limit is not essential and there should be

a simple macroscopic way of developing a numerical scheme which inherits the main features of LBM. The mesh described in the previous section naturally suggests to consider as an alternative a numerical scheme based on finite difference (FD).

Obviously it is possible to design a FD scheme which mimics the leading terms of the macroscopic equations derived by means of the asymptotic analysis up to some degree of accuracy (depending on the considered stencil). However the problem is that the regular expansions used in the previous section involve an infinite number of terms. For this reason, it is impossible to define a finite difference scheme which is perfectly equivalent, at any order of the expansion parameter ϵ, with an LBM scheme. With the expression perfectly equivalent, we intend two schemes producing results which differ each other for difference smaller than the machine precision. With other words, it seems impossible to express the dynamics of the distribution function ruled by the kinetic formulation in terms of a finite number of nodal values of the macroscopic variables, as expected by any FD scheme, because this would be equivalent to express the kinetic dynamics in terms of a closed function of the local equilibrium. Even though the kinetic theory prescribes that the kinetic formulation is infinitesimally close to the local equilibrium in the low Mach number limit, it is not perfectly equivalent to a pure macroscopic formulation, at least in principle. This is displayed also by the closeness of LBM to the kinetic schemes. The kinetic schemes also use the Boltzmann equation of kinetic theory as the starting point, but they are aimed at solving the macroscopic equations of fluid flow. The basic idea is to use the leading terms of the expansion reported in Section 2 in approximating the distribution function in order to derive explicit formula for the numerical fluxes.

Actually since LBM is a discrete nodal algorithm, it is possible to find out a degenerate case. The so-called lattice kinetic scheme (LKS) [13, 14], obtained in case $\lambda = 1$, employs a simpler updating rule of the distribution function than the original LBM. The updated distribution function is given by the linear combination of the equilibrium distribution function, which is characterized by macroscopic variables. It is obvious from this updating rule that LKS deals with only macroscopic variables in the actual computation. In fact, the similarity of LBM with the artificial compressibility method proposed by Chorin [15] is discussed by using LKS in Ref. [14]. From the numerical point of view, there is some room for the improvement of the existing LKS.

(1) The existing LKS employs a larger stencil than that of LBM, which is not advantageous in the actual parallel computation since it requires larger time for data transmission.
(2) Another improvement is expected in the increase of the stability by recognizing LKS as the finite difference method and applying a semi-implicit formulation.

In case $\lambda = 1$ the updating rule Eq. (61) becomes

$$F^+ = F(t + \epsilon^2, x_i, V_i) = F_e(t, x_i - V_i\epsilon, V_i), \tag{111}$$

The equilibrium distribution function F_e is directly based on the hydrodynamic quantities. This allows one to derive a perfectly equivalent FD scheme, based only on macroscopic variables. This FD scheme can be used instead of LKS in order to update the hydrodynamic quantities in time.

Taking the hydrodynamic moments of Eq. (111) yields, for the pressure update in time, i.e. for calculating the pressure at the new time step $p^+ = p(t+\epsilon^2, x_i)$,

$$\begin{aligned} p^+ = p &- \frac{1}{3}\left[\delta_x u_1 + \delta_y u_2 + \frac{\epsilon^2}{6}(\delta_x^2\delta_y u_2 + \delta_x\delta_y^2 u_1)\right] \\ &+\frac{\epsilon^2}{6}\left[\delta_x^2 p + \delta_y^2 p + \delta_x^2(u_1^2) + \delta_y^2(u_2^2) + 2\,\delta_x\delta_y(u_1u_2)\right] \\ &+\frac{\epsilon^4}{36}\,\delta_x^2\delta_y^2\left(p + u_1^2 + u_2^2\right). \end{aligned} \tag{112}$$

For the velocity update in time, i.e. for calculating the velocity components at the new time step $u_1^+ = u_1(t + \epsilon^2, x_i)$ and $u_2^+ = u_2(t + \epsilon^2, x_i)$,

$$\begin{aligned} u_1^+ = u_1 &+ \epsilon^2\left[-\delta_x p - \delta_x(u_1^2) - \delta_y(u_1u_2)\right. \\ &\left.+\frac{\epsilon^2}{12}\,\delta_x^2\delta_y^2 u_1 + \frac{1}{6}\,(3\,\delta_x^2 u_1 + 2\,\delta_x\delta_y u_2 + \delta_y^2 u_1)\right] \\ &-\epsilon^4\left[\frac{1}{6}\,\delta_x\delta_y^2(p + u_1^2 + u_2^2) + \frac{1}{2}\,\delta_x^2\delta_y(u_1u_2)\right], \end{aligned} \tag{113}$$

$$\begin{aligned} u_2^+ = u_2 &+ \epsilon^2\left[-\delta_y p - \delta_y(u_2^2) - \delta_x(u_2u_1)\right. \\ &\left.+\frac{\epsilon^2}{12}\,\delta_y^2\delta_x^2 u_2 + \frac{1}{6}\,(3\,\delta_y^2 u_2 + 2\,\delta_y\delta_x u_1 + \delta_x^2 u_2)\right] \\ &-\epsilon^4\left[\frac{1}{6}\,\delta_y\delta_x^2(p + u_2^2 + u_1^2) + \frac{1}{2}\,\delta_y^2\delta_x(u_2u_1)\right]. \end{aligned} \tag{114}$$

In the previous expressions, the second-order central finite difference formulas δ_x, δ_y, δ_x^2 and δ_y^2 are used in order to collect the linear combinations of the nodal values (see Appendix C for details). The important comment is that the previous expressions are identical operative alternatives to the original LKS scheme. Eqs. (112, 113, 114) are exact, in the sense that they are perfectly equivalent to the numerical scheme defined by Eq. (111).

The leading term in the right hand side of Eq. (112) is clearly related to the divergence of the velocity field. Recalling that, in the low Mach number limit,

$$\delta_x u_1 + \delta_y u_2 + \frac{\epsilon^2}{6}(\delta_x^2 \delta_y u_2 + \delta_x \delta_y^2 u_1) = \frac{\partial u_1}{\partial x} + \frac{\partial u_2}{\partial y} + O(\epsilon^4), \tag{115}$$

then Eq. (112) is clearly a simple implementation of the artificial compressibility method (ACM). It is worth the effort to point out that in this case the ACM is used to recover approximations of the transient ICNS solutions.

Clearly LKS is solving, with second order accuracy in space, the incompressible Navier-Stokes system of equations with an effective kinematic viscosity $\nu = 1/6$, purely due to the numerical discretization error. In the case of the simple LKS scheme, the kinematic viscosity is fixed.

4.1 Compact formulation

The simple LKS scheme can be modified in order to deal with a tunable kinematic viscosity [13]. Recalling the connection between LBM and kinetic schemes, Junk [14] defined a purely finite difference scheme by calculating the leading terms of Chapman-Enskog expansion, the spatial gradients of which are computed by means of central difference formula. The same idea was used in order to improve LKS [34]. Moreover modifying even further the Chapman-Enskog expansion is possible to include additional effects directly in terms of macroscopic variables. In this case, we can take advantage of the analysis reported in Section 2.

The modified updating rule for LKSν becomes

$$F_*^+ = F(t + \epsilon^2, x_i, V_i) = F_{e*}(t, x_i - V_i\epsilon, V_i), \tag{116}$$

where

$$F_{e*} = F_e + \epsilon\tau\partial_S F_e = F_e + \epsilon\tau(V_1\partial_x F_e + V_2\partial_y F_e). \tag{117}$$

The modified local equilibrium F_{e*} involves first order spatial gradients, which are usually approximated by means of central difference operators (see Appendix C for details). However using a central difference approximation in order to compute the spatial gradients in Eq. (117) is equivalent to consider a stencil larger than the original $D2Q9$. Actually it is possible to develop a numerical scheme which is equivalent to LKSν, but it is purely formulated in terms of macroscopic variables and it is based on finite difference formulas (FD-LKSν).

Let us consider an example in order to clarify this concept. Let us consider the following east-west velocity pair of the $D2Q9$ lattice, i.e. $(V_1, V_2)_E = (1, 0) =$

$-(V_1, V_2)_W = (-1, 0)$. In this case, Eq. (117) applied in the W point of the stencil clearly involves the terms $\partial_x u_1(x-\epsilon, y)$ and $\partial_y u_1(x-\epsilon, y)$ which must be computed numerically with second order accuracy. This can be done in the following way

$$\frac{u_1(x-\epsilon, y+\epsilon) - u_1(x-\epsilon, y-\epsilon)}{2\,\epsilon} = \frac{\partial u_1(x-\epsilon, y)}{\partial y} + O(\epsilon^2), \tag{118}$$

$$\frac{-3\,u_1(x-\epsilon, y) + 4\,u_1(x, y) - u_1(x+\epsilon, y)}{2\,\epsilon} = \frac{\partial u_1(x-\epsilon, y)}{\partial x} + O(\epsilon^2). \tag{119}$$

Clearly the first formula is a central difference formula, while the second one is shifted in order to force the numerical approximation to stay inside the considered stencil. However they both ensure the second order accuracy with respect to ϵ. The previous example proves that F_{e*} can be computed purely in terms of macroscopic hydrodynamic quantities by means of proper finite difference interpolation formulas with the required accuracy and this leads to a FD difference scheme, that we will call FD-LKSν.

Following this idea and integrating the kinetic updating rule given by Eq. (116) yields

$$\begin{aligned} p_*^+(p, u_1, u_2) = p - \frac{1}{3}\Bigg[&(\delta_x u_1 + \delta_y u_2)\,(1+\zeta) + \frac{\epsilon^2}{6}(\delta_x^2\delta_y u_2 + \delta_x\delta_y^2 u_1)\Bigg] \\ &+\frac{\epsilon^2}{6}\Bigg[\delta_x^2 p + \delta_y^2 p + \delta_x^2(u_1^2) + \delta_y^2(u_2^2) + 2\,\delta_x\delta_y(u_1 u_2) \\ &-\zeta\,\left(\delta_x^2\delta_y u_2 + \delta_x\delta_y^2 u_1\right)\Bigg] + \frac{\epsilon^4}{36}\,\delta_x^2\delta_y^2\left(p + u_1^2 + u_2^2\right), \end{aligned} \tag{120}$$

where $\zeta = (1-\lambda)/\lambda$, while, for the velocity update in time,

$$\begin{aligned} u_{1*}^+(p, u_1, u_2) = u_1 + \epsilon^2\Bigg[&-\delta_x p - \delta_x(u_1^2) - \delta_y(u_1 u_2) \\ &+\frac{\epsilon^2}{3}\,\left(\frac{1}{4} + \zeta\right)\,\delta_x^2\delta_y^2 u_1 + \nu\,(3\,\delta_x^2 u_1 + 2\,\delta_x\delta_y u_2 + \delta_y^2 u_1)\Bigg] \\ &-\epsilon^4\,\left[\frac{1}{6}\,\delta_x\delta_y^2(p + u_1^2 + u_2^2) + \frac{1}{2}\,\delta_x^2\delta_y(u_1 u_2)\right], \end{aligned} \tag{121}$$

$$u_{2*}^{+}(p,u_1,u_2) = u_2 + \epsilon^2 \left[-\delta_y p - \delta_y(u_2^2) - \delta_x(u_2 u_1) \right.$$
$$\left. + \frac{\epsilon^2}{3} \left(\frac{1}{4} + \zeta \right) \delta_y^2 \delta_x^2 u_2 + \nu \left(3\,\delta_y^2 u_2 + 2\,\delta_y \delta_x u_1 + \delta_x^2 u_2 \right) \right]$$
$$- \epsilon^4 \left[\frac{1}{6}\,\delta_y \delta_x^2 (p + u_2^2 + u_1^2) + \frac{1}{2}\,\delta_y^2 \delta_x (u_2 u_1) \right], \qquad (122)$$

where the kinematic viscosity is

$$\nu = \frac{1}{3} \left(\frac{1}{2} + \zeta \right) = \frac{1}{3} \left(\frac{1}{\lambda} - \frac{1}{2} \right). \qquad (123)$$

As in the previous section, the second order finite difference formulas are used in order to collect the linear combinations of the nodal values (see Appendix C for details).

Clearly the FD-LKSν solves the incompressible Navier-Stokes system of equations with tunable kinematic viscosity ν. This section is consistent with the previous one, because, in case of $\zeta = 0$, the results for simple FD-LKS are recovered. The idea of using non-central difference formulas for the calculation of the spatial gradient of the regular expansion without reducing the accuracy of the original LKSν scheme allows one to define a practical alternative FD scheme, purely based on macroscopic variables. Preliminary results seem to suggest that FD-LKSν is stable for $1 \leq \lambda < 2$.

4.2 Semi-implicit formulation

In this section, the previous formula for p_*^+, u_{1*}^+ and u_{2*}^+ will be used to derive a semi-implicit scheme. Essentially once the operative updating formulas are expressed in terms of macroscopic variables, it is possible to apply first those for the velocity components in order to compute the new values (explicitly), then it is possible to use this updated velocity field at the new time step in order to compute a consistent pressure field (implicitly). This simple approach is very common in CFD community, but it is not possible in the simple formulations of LKS because this scheme considers as unknowns only the discrete distribution functions. Let us summarize the semi-implicit algorithm.

- Let us start with p, u_1 and u_2 at $t = t_1$.
- Let us compute $u_{1*}^+(p,u_1,u_2)$ and $u_{2*}^+(p,u_1,u_2)$ (explicit step).
- Let us compute $p_*^+(p,u_{1*}^+,u_{2*}^+)$ by using the new values for the velocity components (implicit step).
- Let us compute $p_*^+ \to p$, $u_{1*}^+ \to u_1$ and $u_{2*}^+ \to u_2$ at $t = t_2 = t_1 + \delta t$.

Clearly the implementation of the previous idea for a scheme formulated in terms of macroscopic variables is very simple.

5 NUMERICAL RESULTS

In this section, some numerical results are reported in order to verify: (a) the validity of the expressions for the coefficients of the asymptotic expansion, given by Eqs. (71-76) and (b) to compare preliminarily the numerical results by FD-LKSν with conventional schemes.

Let us consider the two-dimensional (2D) standing Taylor-Green vortex flow as a test case. Let us consider a square domain $(x, y) \in [0, 6] \times [0, 6]$. The standing Taylor-Green vortex flow has the following analytic solutions to the incompressible Navier-Stokes equation in two dimensions:

$$u_1(t, x, y) = -\cos\left(\frac{\pi x}{3}\right) \sin\left(\frac{\pi y}{3}\right) \exp\left(-\frac{2\pi^2 \nu t}{9}\right), \tag{124}$$

$$u_2(t, x, y) = \cos\left(\frac{\pi y}{3}\right) \sin\left(\frac{\pi x}{3}\right) \exp\left(-\frac{2\pi^2 \nu t}{9}\right), \tag{125}$$

$$p(t, x, y) = -\frac{1}{4}\left[\cos\left(\frac{2\pi x}{3}\right) + \cos\left(\frac{2\pi y}{3}\right)\right] \exp\left(-\frac{4\pi^2 \nu t}{9}\right). \tag{126}$$

5.1 Validation of asymptotic analysis

In order to verify the validity of the expressions for the coefficients of the asymptotic expansion, given by Eqs. (71-76), let us define first the following quantity

$$F^{[k]} = \sum_{i=0}^{k} \epsilon^k \, F^{(k)}. \tag{127}$$

According to the assumptions of the asymptotic analysis $F^{[k]} - F = O(\epsilon^{k+1})$ and this theoretical trend can be verified by considering different discretization steps ϵ for the test case. Analogously we can define $\rho^{[k]}$ and $u_i^{[k]}$. Then we use the previous approximations in order to derive macroscopic equations approximating the behavior of the numerical scheme, namely

$$\langle F^{[k]} - F_e^{[k]} \rangle = \partial_t \rho^{[k]} + \mathrm{Eq}_\rho^{[k]}(\rho^{[k]}, u_j^{[k]}) = 0, \tag{128}$$

$$\langle V_i \, (F^{[k]} - F_e^{[k]}) \rangle = \partial_t {u_i}^{[k]} + \mathrm{Eq}_u^{[k]}(\rho^{[k]}, u_j^{[k]}) = 0. \tag{129}$$

Recalling that $\partial_\alpha \rho = O(\epsilon^2)$ and $\partial_\alpha u_j = O(\epsilon)$ where $\alpha = t, x_i$, then it is possible to prove that $\partial_t \rho + \mathrm{Eq}_\rho^{[k]}(\rho, u_j) = O(\epsilon^{k+3})$ and $\partial_t u + \mathrm{Eq}_u^{[k]}(\rho, u_j) = O(\epsilon^{k+2})$, if ρ and u_j are numerical solutions of LBM scheme.

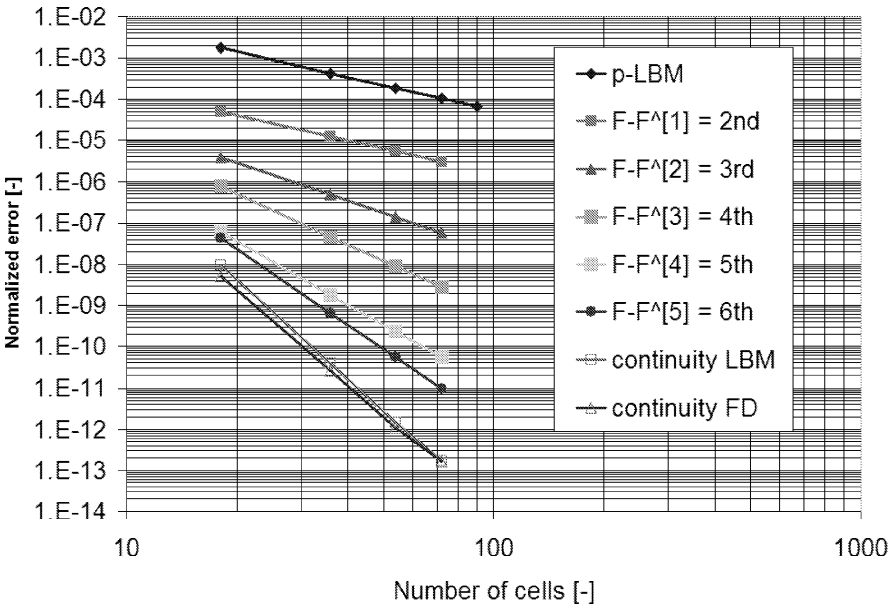

Fig. 1. Two-dimensional (2D) standing Taylor-Green vortex flow. Numerical verification of the convergence rate of $F - F^{[k]} = O(\epsilon^{k+1})$ for $k = 1, 2, 3, 4, 5$ and the consequent approximation for the continuity equation $\partial_t \rho + \mathrm{Eq}_\rho^{[5]}(\rho, u_j) = O(\epsilon^8)$.

In Figs. 1 and 2 the numerical verification of the convergence rate of $F - F^{[k]} = O(\epsilon^{k+1})$ for $k = 1, 2, 3, 4, 5$ is reported for the two-dimensional (2D) standing Taylor-Green vortex flow. In particular, in Fig. 1 the fifth order FD approximation of the continuity equation $\partial_t \rho + \mathrm{Eq}_\rho^{[5]}(\rho, u_j) = O(\epsilon^8)$ is reported. On the other hand, in Fig. 2 the fifth order FD approximation of the momentum equation $\partial_t u_1 + \mathrm{Eq}_u^{[5]}(\rho, u_j) = O(\epsilon^7)$ is reported. Both the verification based on the discrete distribution function and that based on the macroscopic equations recovered by the scheme produced accurate results.

5.2 Artificial compressibility method

Before considering the improved LKS, called FD-LKSν, designed in Section 4, we derived a simpler scheme based on the artificial compressibility method (ACM). It is possible to define an ACM by neglecting the errors $\sim O(\epsilon^2)$ only in Eq. (110), namely

$$\frac{\partial u_i}{\partial t} + u_j \frac{\partial u_i}{\partial x_j} + \frac{\partial p}{\partial x_i} = \nu \frac{\partial^2 u_i}{\partial x_j^2}. \tag{130}$$

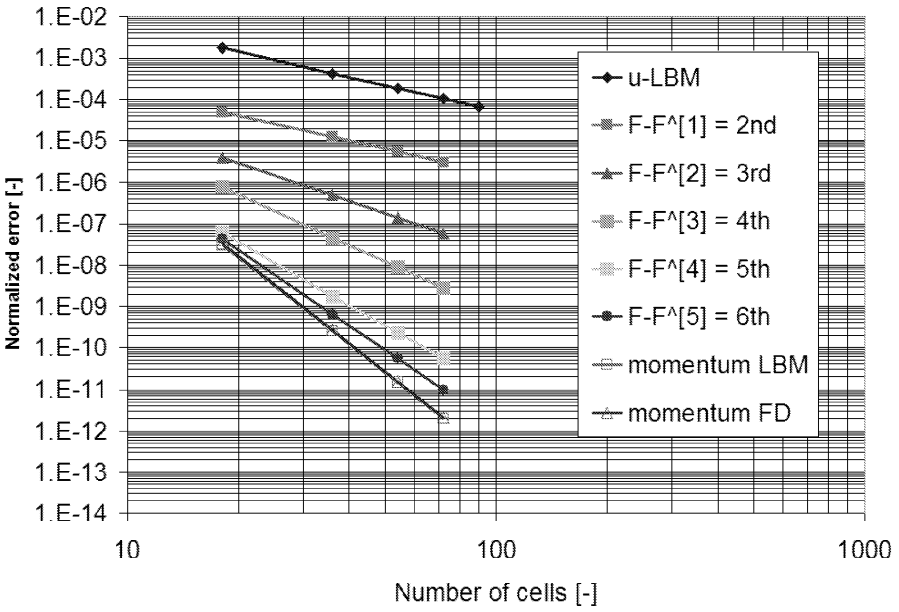

Fig. 2. Two-dimensional (2D) standing Taylor-Green vortex flow. Numerical verification of the convergence rate of $F - F^{[k]} = O(\epsilon^{k+1})$ for $k = 1, 2, 3, 4, 5$ and the consequent approximation for the momentum equation $\partial_t u_1 + \mathrm{Eq}_u^{[5]}(\rho, u_j) = O(\epsilon^7)$.

The system of equations (103, 130) can be solved by means of any efficient FD scheme. Obviously pure central difference approximations of the previous system is not a good idea, since they lead to unstable schemes because of the chessboard pressure problem, which can be solved by staggered grids. However operative formula Eq. (112, 113, 114) may suggest better discretization strategies, since preliminary results seem to suggest that they are stable for $\delta t \leq \delta t_0$, where $\delta t_0 = \epsilon^2/(6\,\nu)$. The key point is that macroscopic equations derived by LKS may be used in order to lead the discretization process and to overcome the chessboard pressure problem on simple non-staggered grids.

To define the best discretization of Eqs. (103, 130) in terms of stability is a very difficult task, because the concept itself of stability for non-linear systems depends somehow on the considered application. One possible choice is the following

$$p^+_{**} = p - \frac{1}{3}\left[\delta_x u_1 + \delta_y u_2 + \frac{\epsilon^2}{6}(\delta_x^2 \delta_y u_2 + \delta_x \delta_y^2 u_1)\right], \tag{131}$$

$$u^+_{1**} = u_1 + \epsilon^2\left[-\delta_x p - \delta_x(u_1^2) - \delta_y(u_1 u_2) + \nu\left(\delta_x^2 u_1 + \delta_y^2 u_1\right) + \frac{\epsilon^2}{2}\,\nu\,\delta_x^2\delta_y^2 u_1\right], \tag{132}$$

$$u^+_{2**} = u_2 + \epsilon^2\left[-\delta_y p - \delta_y(u_2^2) - \delta_x(u_2 u_1) + \nu\left(\delta_y^2 u_2 + \delta_x^2 u_2\right) + \frac{\epsilon^2}{2}\,\nu\,\delta_y^2\delta_x^2 u_2\right], \tag{133}$$

which we will call ACM. In particular, the last terms in Eqs. (132, 133) allow

one to highly increase the stability region of the original scheme, which was actually as small as that of a pure central difference scheme. Analogously to what done in the previous section, it is possible to introduce a semi-implicit formulation by computing first the new velocity components $u^+_{1**}(p, u_1, u_2)$ and $u^+_{2**}(p, u_1, u_2)$, and then use them in order to update the pressure field, i.e. $p^+_{**}(p, u^+_{1**}, u^+_{2**})$. This numerical trick will be used in the numerical simulations. Preliminary results seem to suggest that ACM is stable for $0 < \nu \leq 1/6$.

5.3 Improved LKS at work

In this section, the previously discussed numerical scheme will be compared in solving the test case. Concerning the stability region of the FD schemes, some preliminary results seem to suggest that FD-LKSν and ACM are stable for $1 \leq \lambda < 2$ and $0 < \nu \leq 1/6$ respectively. It is worth the effort to point out that, recalling Eq. (123), selecting λ in FD-LKSν such as $1 \leq \lambda < 2$ implies an actual kinematic viscosity $0 < \nu \leq 1/6$. Consequently both FD schemes seem stable for $0 < \nu \leq 1/6$. On the other hand, LBM schemes are stable for $0 < \lambda < 2$, which implies only $\nu > 0$. This seems to prove that there is a contraction of the stability region of FD schemes in comparison with the original LBM schemes. However the portion $0 < \nu \leq 1/6$ is the domain relevant for most of the applications: for this reason, the previous stability contraction does not seem a serious issue.

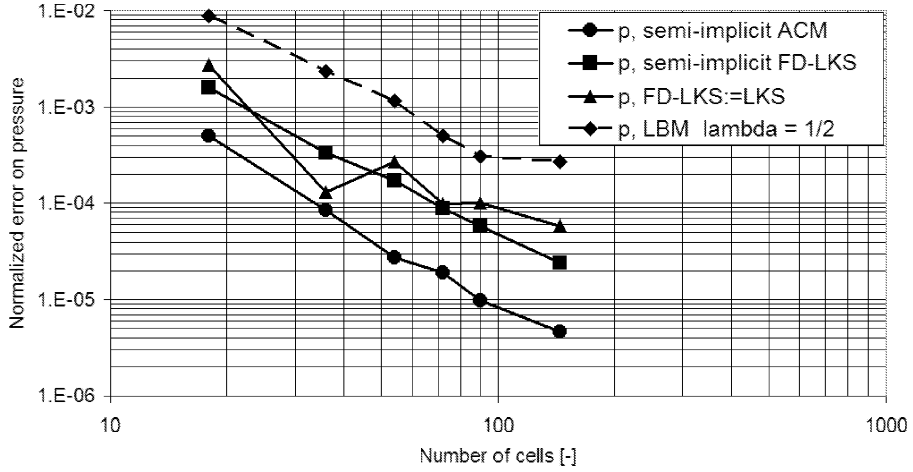

Fig. 3. Two-dimensional (2D) standing Taylor-Green vortex flow. Comparison of convergence rate for the pressure field among different numerical schemes (semi-implicit ACM method, semi-implicit FD-LKS, LKS and LBM method).

In the following calculations, the maximum time step was used for the FD schemes, i.e. $\lambda = 1$. Strictly speaking, this means that LKS and FD-LKS were considered. Similar considerations apply for FD-LKSν. In Fig. 3, comparison of convergence rate for the pressure field among different numerical

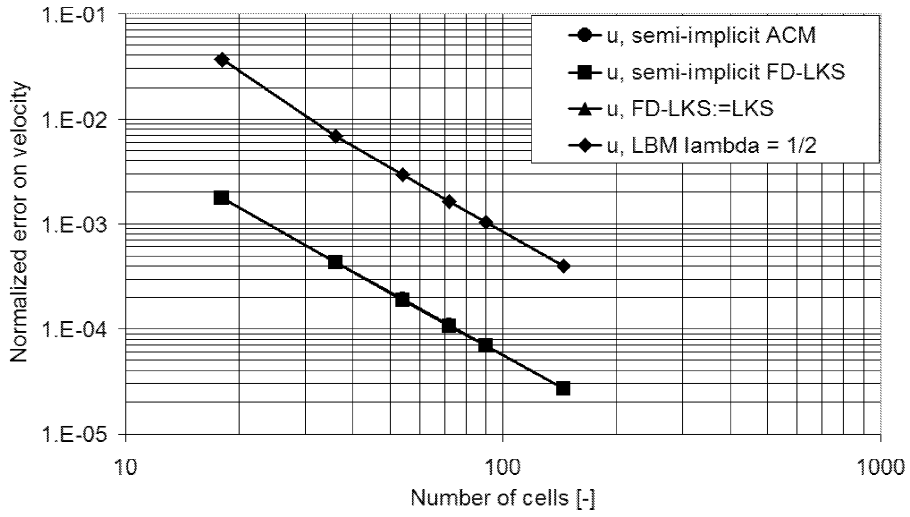

Fig. 4. Two-dimensional (2D) standing Taylor-Green vortex flow. Comparison of convergence rate for the velocity field among different numerical schemes (semi-implicit ACM method, semi-implicit FD-LKS, LKS and LBM method).

schemes (semi-implicit ACM method, semi-implicit FD-LKS, LKS and LBM method) is reported. The comparison in terms of the convergence rate for the pressure field is reported in Fig. 4. The latter field is solved in a way substantially equivalent by the first three schemes (semi-implicit ACM method, semi-implicit FD-LKS and LKS), while the possibility for LBM to consider larger time steps and smaller dimensionless relaxation frequencies ($\lambda = 1/2$ in the plot) is compensated by the larger numerical errors generated. The main differences appear in solving the pressure field. LKS and LBM show a non-regular decay, if the discretization accuracy is increased. This is due to parasitic acoustic waves moving in the domain. On the other hand, the decay for the semi-implicit FD-LKS is much more close to the theoretical expectations, even though the smallest numerical errors are achieved by the simple semi-implicit ACM.

Finally, in Fig. 5 a comparison between explicit FD-LKS and LBM for different values of the dimensionless relaxation frequency and of the discretization step is reported, in terms of the numerical errors produced in order to solve the velocity field. Clearly, the two schemes are identical in case of $\lambda = 1$, because explicit FD-LKS $\equiv$ LKS for construction and LKS $\equiv$ LBM in case of $\lambda = 1$. In the range $1 \leq \lambda < 2$ (the only one possible for FD-LKSν), LBM produces always numerical errors which are smaller or eventually equal to those of the explicit FD-LKSν scheme.

These numerical results are preliminary and not exhaustive, however they are enough to prove that the designed FD schemes are not simply theoretical curiosities but they may lead to practical alternatives to LBM. A detailed comparison and an optimized design of the FD schemes will be discussed in a

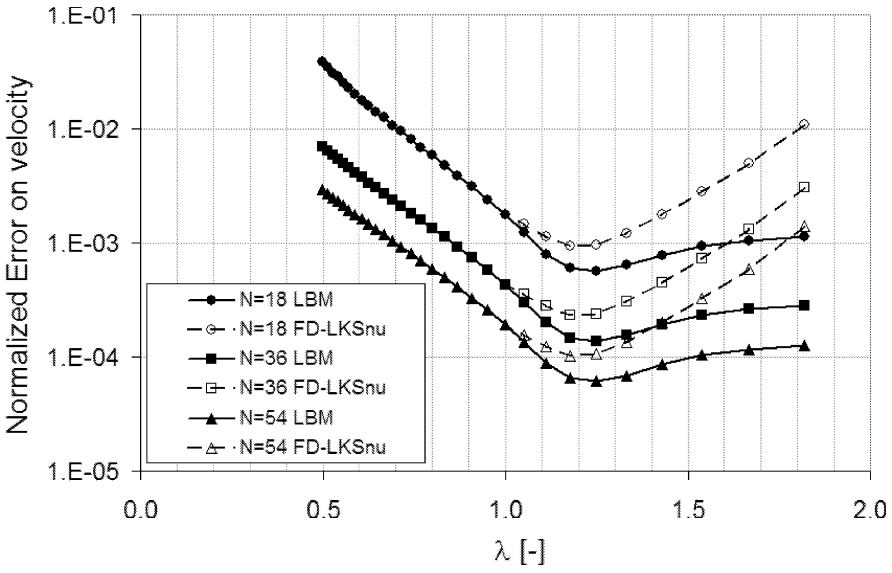

Fig. 5. Two-dimensional (2D) standing Taylor-Green vortex flow. Comparison between FD-LKSν and LBM for different values of the dimensionless relaxation frequency λ and of the discretization step, in terms of the numerical errors produced in order to solve the velocity field.

next paper.

6 CONCLUSIONS

In this section, we summarize the main results of the present paper.

(1) First of all, we discussed the perspective of realization of LBM computation beyond NS. For this purpose, we carry out the asymptotic analysis of discrete BGK equation and lattice-BGK method according to the recipe of Ref. [21], where the asymptotic behavior of MRT-LBM is studied up to NS order only. The principal part of the resulting equation system is in the same form as Chorin's artificial compressibility system. Beyond that, the macroscopic equations recovered by the simple LBM scheme differ from those prescribed by the original kinetic model. This means that simple LBM scheme leads to "non-existing" higher order rarefaction effect. Hence, if special treatments are not considered, and, in particular, larger lattices are not used, it is impossible to claim that the simple LBM scheme may naturally catch physics beyond the NS description of the flow. This fake rarefaction effect becomes more real one, only when the stencil becomes larger.
(2) We derived the principal equation system in a different and simpler manner from the discrete BGK equation by using the Grad moment system.

After introducing a proper scaling of both the kinetic equations and the macroscopic moments according to the regime we are interested in, the macroscopic equations are simply recovered by recursive substitution. This proves that the key point in the derivation of the macroscopic equations is the diffusion scaling and that complex expansions of the hydrodynamic conserved moments can be avoided. This approach allows one to make simpler the analysis of existing schemes and the design of new ones.

(3) Finally, we improved the existing LKS scheme in the efficiency and stability on the basis of the fact that it deals with the artificial compressibility system. Essentially two improvements were proposed: first of all, (a) the scheme is formulated purely in terms of macroscopic quantities on a compact stencil; secondly (b) the semi-implicit formulation is proposed in order to increase the actual stability of the scheme. The LBM, LKS, and the improved LKS, called FD-LKSν, were tested in the standing Taylor-Green problem.

7 Acknowledgments

A part of the first author's work (P. A.) was done during his visit to Kyoto University. His stay was supported by the project "New approach in computational fluid dynamics on the basis of kinetic theory" within the fund "Grants-in-Aid for Scientific Research No. 175600147" from Japan Society for the Promotion of Science and the 21st Century COE Program: Center of Excellence for Research and Education on Complex Functional Mechanical Systems from Ministry of Education, Culture, Sports, Science and Technology - JAPAN.

A APPENDIX

In this Appendix, some more details are reported on how to derive Eqs.(34, 35). In particular for $k = 5$, Eq.(27) yields

$$\langle\langle \phi \left[\partial_t f^{(3)} + \partial_s f^{(4)} \right] \rangle\rangle = 0, \tag{A.1}$$

or equivalently

$$\langle\langle \phi \left\{ \partial_t f_e^{(3)} + \partial_s f_e^{(4)} - \tau \left[\partial_t^2 f_e^{(1)} + 2\,\partial_t \partial_s f_e^{(2)} + \partial_s^2 f_e^{(3)} \right] \right.$$
$$\left. + \tau^2 \left[2\,\partial_t^2 \partial_s f_e^{(0)} + 3\,\partial_t \partial_s^2 f_e^{(1)} + \partial_s^3 f_e^{(2)} \right] - \tau^3 \left[\partial_t \partial_s^3 f_e^{(0)} + \partial_s^4 f_e^{(1)} \right] \right\} \rangle\rangle = 0. \tag{A.2}$$

Selecting first $\phi = 1$, the elementary integrals involved in the previous expression are

$$\langle\langle \partial_s f_e^{(4)} \rangle\rangle = \frac{\partial q_i^{(4)}}{\partial x_i},$$
$$\langle\langle \partial_s f_e^{(2)} \rangle\rangle = \frac{\partial u_i^{(2)}}{\partial x_i} = 0, \tag{A.3}$$
$$\langle\langle \partial_s f_e^{(0)} \rangle\rangle = 0,$$
$$\langle\langle \partial_s^2 f_e^{(3)} \rangle\rangle = \frac{\partial^2 p^{(3)}}{\partial x_k^2} + \frac{\partial^2}{\partial x_i \partial x_j}(u_i^{(1)} u_j^{(2)} + u_i^{(2)} u_j^{(1)}) = 0, \tag{A.4}$$
$$\langle\langle \partial_s^2 f_e^{(1)} \rangle\rangle = \frac{\partial^2 p^{(1)}}{\partial x_k^2} = 0, \tag{A.5}$$
$$\langle\langle \partial_s^3 f_e^{(2)} \rangle\rangle = \frac{\partial^3 u_i^{(2)}}{\partial x_k^2 \partial x_i} = 0, \tag{A.6}$$
$$\langle\langle \partial_s^3 f_e^{(0)} \rangle\rangle = 0,$$
$$\langle\langle \partial_s^4 f_e^{(1)} \rangle\rangle = \frac{\partial^4 p^{(1)}}{\partial x_k^2 \partial x_j^2} = 0. \tag{A.7}$$

In particular, the conditions (41) have been applied. Introducing the previous intermediate terms in Eqs. (A.2) yields

$$\frac{\partial q_i^{(4)}}{\partial x_i} = 0. \tag{A.8}$$

In a similar way, selecting $\phi = v_i$, the following elementary integrals appear

$$\langle\langle \partial_s f_e^{(4)}\, v_i \rangle\rangle = \frac{\partial p^{(4)}}{\partial x_i} + \frac{\partial}{\partial x_j}(u_i^{(1)} q_j^{(3)} + q_i^{(3)} u_j^{(1)}),$$

$$\langle\langle \partial_s f_e^{(2)}\, v_i \rangle\rangle = \frac{\partial p^{(2)}}{\partial x_i} + \frac{\partial}{\partial x_j}(u_i^{(1)} u_j^{(1)}),$$

$$\langle\langle \partial_s f_e^{(0)}\, v_i \rangle\rangle = 0,$$

$$\langle\langle \partial_s^2 f_e^{(3)}\, v_i \rangle\rangle = 1/3\, \frac{\partial^2 q_i^{(3)}}{\partial x_k^2} + 2/3\, \frac{\partial^2 q_j^{(3)}}{\partial x_i \partial x_j} + \frac{\partial^2}{\partial x_k \partial x_j}(u_i^{(1)} u_j^{(1)} u_k^{(1)}), \tag{A.9}$$

$$\langle\langle \partial_s^2 f_e^{(1)}\, v_i \rangle\rangle = 1/3\, \frac{\partial^2 u_i^{(1)}}{\partial x_k^2},$$

$$\langle\langle \partial_s^3 f_e^{(2)}\, v_i \rangle\rangle = \frac{\partial^3}{\partial x_k^2 \partial x_j}(u_i^{(1)} u_j^{(1)}), \tag{A.10}$$

$$\langle\langle \partial_s^3 f_e^{(0)}\, v_i \rangle\rangle = 0,$$

$$\langle\langle \partial_s^4 f_e^{(1)}\, v_i \rangle\rangle = 1/3\, \frac{\partial^4 u_i^{(1)}}{\partial x_k^2 \partial x_j^2}. \tag{A.11}$$

Again introducing the previous results in Eqs. (A.2) yields, after some algebra,

$$\frac{\partial q_i^{(3)}}{\partial t} + \frac{\partial}{\partial x_j}(u_i^{(1)} q_j^{(3)} + q_i^{(3)} u_j^{(1)}) + \frac{\partial p^{(4)}}{\partial x_i} = \tau/3\, \frac{\partial^2 q_i^{(3)}}{\partial x_k^2} + \tau/3\, \frac{\partial^2 q_j^{(3)}}{\partial x_i \partial x_j} + i_3, \tag{A.12}$$

where i_3 is defined as

$$\begin{aligned} i_3 = {} & \tau \frac{\partial}{\partial x_j} \left[\frac{\tau}{3} \frac{\partial^2 u_i^{(1)}}{\partial x_k^2} - \frac{\partial u_i^{(1)}}{\partial x_k} u_k^{(1)} - \frac{\partial p^{(2)}}{\partial x_i} \right] u_j^{(1)} \\ & + \tau \frac{\partial u_i^{(1)}}{\partial x_j} \left[\frac{\tau}{3} \frac{\partial^2 u_j^{(1)}}{\partial x_k^2} - \frac{\partial u_j^{(1)}}{\partial x_k} u_k^{(1)} - \frac{\partial p^{(2)}}{\partial x_j} \right] + \tau \frac{\partial^2}{\partial x_k \partial x_j}(u_i^{(1)} u_j^{(1)} u_k^{(1)}) \\ & + 2\, \frac{\tau^2}{3}\, \frac{\partial^3 p^{(2)}}{\partial x_k^2 \partial x_i} - \frac{\tau^2}{3}\, \frac{\partial}{\partial x_k^2} \left[\frac{\partial u_i^{(1)}}{\partial x_j} u_j^{(1)} \right] + \frac{\tau^3}{9}\, \frac{\partial^4 u_i^{(1)}}{\partial x_k^2 \partial x_j^2}, \end{aligned} \tag{A.13}$$

and clearly it depends on the lower order coefficients only.

B APPENDIX

In this Appendix, some more details are reported on how to derive Eqs.(85). As discussed in Appendix A, the key point is how to compute the elementary integrals involved in the approximated expressions derived by means of the asymptotic analysis. Let us derive the corresponding integrals for the discrete case, namely

$$
\begin{aligned}
\langle \partial_S F_e^{(4)} V_i \rangle &= \frac{\partial p^{(4)}}{\partial x_i} + \frac{\partial}{\partial x_j}(u_i^{(1)} q_j^{(3)} + q_i^{(3)} u_j^{(1)}),\\
\langle \partial_S F_e^{(2)} V_i \rangle &= \frac{\partial p^{(2)}}{\partial x_i} + \frac{\partial}{\partial x_j}(u_i^{(1)} u_j^{(1)}),\\
\langle \partial_S F_e^{(0)} V_i \rangle &= 0,\\
\langle \partial_S^2 F_e^{(3)} V_i \rangle &= 1/3\, \frac{\partial^2 q_i^{(3)}}{\partial x_k^2} + 2/3\, \frac{\partial^2 q_j^{(3)}}{\partial x_i \partial x_j}, \qquad \text{(B.1)}\\
\langle \partial_S^2 F_e^{(1)} V_i \rangle &= 1/3\, \frac{\partial^2 u_i^{(1)}}{\partial x_k^2},\\
\langle \partial_S^3 F_e^{(2)} V_i \rangle &= \frac{\partial^3}{\partial x_k^2 \partial x_j}(u_i^{(1)} u_j^{(1)}) - \frac{\partial^3 (u_i^{(1)})^2}{\partial x_i^3}, \qquad \text{(B.2)}\\
\langle \partial_S^3 F_e^{(0)} V_i \rangle &= 0,\\
\langle \partial_S^4 F_e^{(1)} V_i \rangle &= 1/3\, \frac{\partial^4 u_i^{(1)}}{\partial x_k^2 \partial x_j^2} - 2/3\, \frac{\partial^4 u_i^{(1)}}{\partial x_i^4}. \qquad \text{(B.3)}
\end{aligned}
$$

Comparing the previous expressions with those for the continuous case, the limits of the terms derived for the simple LBM scheme are evident. By comparing Eq. (B.1) with Eq. (A.9), it is evident that the usual equilibrium distribution function [27], truncated up to the second order, does not allow one to derive third order terms in the previous integrals. Secondly by comparing Eqs. (B.2, B.3) with Eqs. (A.10, A.11), the former show a lack of symmetry, since the last terms in the right hand side cannot be expressed in terms of the classical differential operators.

$$
\frac{\partial q_i^{(3)}}{\partial t} + \frac{\partial}{\partial x_j}(u_i^{(1)} q_j^{(3)} + q_i^{(3)} u_j^{(1)}) + \frac{\partial p^{(4)}}{\partial x_i} = \omega_1/3\, \frac{\partial^2 q_i^{(3)}}{\partial x_k^2} + \omega_1/3\, \frac{\partial^2 q_j^{(3)}}{\partial x_i \partial x_j} + I_3, \quad \text{(B.4)}
$$

where I_3 is defined as

$$
\begin{aligned}
I_3 = {} & \omega_1 \frac{\partial}{\partial x_j} \left[\frac{\omega_1}{3}\, \frac{\partial^2 u_i^{(1)}}{\partial x_k^2} - \frac{\partial u_i^{(1)}}{\partial x_k} u_k^{(1)} - \frac{\partial p^{(2)}}{\partial x_i} \right] u_j^{(1)}\\
& + \omega_1 \frac{\partial u_i^{(1)}}{\partial x_j} \left[\frac{\omega_1}{3}\, \frac{\partial^2 u_j^{(1)}}{\partial x_k^2} - \frac{\partial u_j^{(1)}}{\partial x_k} u_k^{(1)} - \frac{\partial p^{(2)}}{\partial x_j} \right]\\
& + (\omega_2 - \omega_1^2/3)\, \frac{\partial^3 p^{(2)}}{\partial x_k^2 \partial x_i} + (\omega_3/3 - \omega_1\omega_2/3 + \omega_1^3/9)\, \frac{\partial^4 u_i^{(1)}}{\partial x_k^2 \partial x_j^2}\\
& - \frac{\omega_1^2}{3}\, \frac{\partial}{\partial x_k^2} \left[\frac{\partial u_i^{(1)}}{\partial x_j} u_j^{(1)} \right] + \omega_2\, \frac{\partial^3 (u_i^{(1)})^2}{\partial x_i^3} - 2\,\omega_3/3\, \frac{\partial^4 u_i^{(1)}}{\partial x_i^4}, \qquad \text{(B.5)}
\end{aligned}
$$

and clearly it depends on the lower order coefficients only.

C APPENDIX

In this appendix, some FD operators are reported for the generic function $\phi(x, y)$, which are linear combinations of the nodal values.

$$\delta_x \phi(x, y) = \frac{\phi(x + \epsilon, y) - \phi(x - \epsilon, y)}{2\,\epsilon}, \tag{C.1}$$

$$\delta_y \phi(x, y) = \frac{\phi(x, y + \epsilon) - \phi(x, y - \epsilon)}{2\,\epsilon}, \tag{C.2}$$

$$\delta_x^2 \phi(x, y) = \frac{\phi(x + \epsilon, y) - 2\,\phi(x, y) + \phi(x - \epsilon, y)}{\epsilon^2}, \tag{C.3}$$

$$\delta_y^2 \phi(x, y) = \frac{\phi(x, y + \epsilon) - 2\,\phi(x, y) + \phi(x, y - \epsilon)}{\epsilon^2}, \tag{C.4}$$

References

[1] G. R. McNamara and G. Zanetti. Use of the lattice Boltzmann to simulate lattice-gas automata. *Phys. Rev. Lett.*, 61:2332–2335, 1988.

[2] F. J. Higuera and J. Jiménez. Boltzmann approach to lattice gas simulations. *Europhys. Lett.*, 9:663–668, 1989.

[3] F. J. Higuera, S. Succi, and R. Benzi. Lattice gas dynamics with enhanced collisions. *Europhys. Lett.*, 9:345–349, 1989.

[4] H. Chen, S. Chen, and H. W. Matthaeus. Recovery of the Navier-Stokes equations using a lattice-gas Boltzmann method. *Phys. Rev. A*, 45:R5339–R5342, 1992.

[5] Y. Qian, D. d'Humières, and P. Lallemand. Lattice BGK models for Navier-Stokes equation. *Europhys. Lett.*, 17:479–484, 1992.

[6] X. He and L.-S. Luo. Theory of lattice Boltzmann method: From the Boltzmann equation to the lattice Boltzmann equation. *Phys. Rev. E*, 56:6811–6817, 1997.

[7] X. Shan and X. He. Discretization of the velocity space in the solution of the Boltzmann equation. *Phys. Rev. Lett.*, 80:65–68, 1998.

[8] D. Wolf-Gladrow. *Lattice-Gas Cellular Automata and Lattice Boltzmann Models.* Number 1725 in Lecture Notes in Mathematics. Springer-Verlag, Berlin, 2nd edition, 2000.

[9] S. Succi. *The Lattice Boltzmann Equation for Fluid Dynamics and Beyond.* Oxford University Press, New York, 2nd edition, 2001.

[10] G.D Doolen (Editor), editor. *Lattice Gas Methods for Partial Differential Equations.* Addison-Wesley, New York, 1990.

[11] R. Benzi, S. Succi, and M. Vergassola. The lattice Boltzmann equation: theory and applications. *Phys. Rep.*, 222:145–197, 1992.

[12] G. D. Doolen S. Chen. Lattice Boltzmann method for fluid flow. *Annu. Rev. Fluid Mech.*, 30:329–364, 1998.

[13] T. Inamuro. A lattice kinetic scheme for incompressible viscous flows with heat transfer. *Proc. R. Soc. Lond. A*, 360(1792):477–484, 2002.

[14] M. Junk. A finite difference interpretation of the lattice Boltzmann method. *Numer. Methods Part. Diff. Eq.*, 17:383–402, 2001.

[15] A. J. Chorin. Numerical solution of the navier-stokes equations. *Mathematics of Computations*, 22:745–762, 1968.

[16] D. I. Pullin. Direct simulation methods for compressible inviscid ideal gas flow. *J. Computat. Phys.*, 34:231, 1980.

[17] S. Y. Chou and D. Baganoff. Kinetic flux-vector splitting for the navier-stokes equations. *J. Computat. Phys.*, 130:217, 1997.

[18] T. Ohwada and S. Kobayashi. Management of discontinuous reconstruction in kinetic schemes. *J. Computat. Phys.*, 197(1):116–38, 2004.

[19] T. Ohwada and S. Fukata. Simple derivation of high-resolution schemes for compressible flows by kinetic approach. *J. Computat. Phys.*, 211:424–447, 2006.

[20] T. Ohwada and K. Xu. The kinetic scheme for the full-burnett equations. *J. Computat. Phys.*, 201(1):315–332, 2004.

[21] M. Junk, A. Klar, and L.-S. Luo. Asymptotic analysis of the lattice Boltzmann equation. *J. Computat. Phys.*, 210(2):676–704, 2005.

[22] S. Chapman and T. G. Cowling. *The Mathematical Theory of Non-Uniform Gases.* Cambridge University Press, Cambridge, UK, 3rd edition, 1970.

[23] C. Cercignani. *The Boltzmann Equation and its Application.* Springer, New York, 1988.

[24] P. L. Bhatnagar, E. P. Gross, and M. Krook. A model for collision processes in gases. I. Small amplitude processes in charged and neutral one-component systems. *Phys. Rev.*, 94:511–525, 1954.

[25] C. Bardos, F. Golse, and C. D. Levermore. Fluid dynamic limits of kinetic equations. I. Formal derivations. *J. Stat. Phys.*, 63:323–344, 1991.

[26] Y. Sone. *Kinetic Theory and Fluid Dynamics.* Birkhäuser, Boston, 2nd edition, 2002.

[27] X. He and L.-S. Luo. Lattice Boltzmann model for the incompressible Navier-Stokes equation. *J. Stat. Phys.*, 88:927–944, 1997.

[28] X. Nie, G.D. Doolen, and S. Chen. Lattice–Boltzmann simulations of fluid flows in mems. *J. Stat. Phys.*, 107(1/2):279–89, 2002.

[29] C. Y. Lim, C. Shua, X. D. Niu, and Y. T. Chew. Application of lattice Boltzmann method to simulate microchannel flows. *Phys. Fluids*, 14(7):2299–308, 2002.

[30] B. Li and D. Y. Kwok. Discrete Boltzmann equation for microfluidics. *Phys. Rev. Lett.*, 90(124502):124502/1-4, 2003.

[31] C. Shen, D. B. Tian, C. Xie, and J. Fan. Examination of the LBM in simulation of microchannel flow in transitional regime. *Microscale Thermophys. Eng.*, 8(4):423–432, 2004.

[32] L.-S. Luo. Comment on "Discrete Boltzmann equation for microfluidics". *Phys. Rev. Lett.*, 92(13):139401/1, 2004.